

## Synthesis and Photophysical Characterization of Porphyrin, Chlorin and Bacteriochlorin Molecules Bearing Tethers for Surface Attachment

Chinnasamy Muthiah<sup>1</sup>, Masahiko Taniguchi<sup>1</sup>, Han-Je Kim<sup>1</sup>, Izabela Schmidt<sup>1</sup>, Hooi Ling Kee<sup>2</sup>, Dewey Holten<sup>\*2</sup>, David F. Bocian<sup>\*3</sup> and Jonathan S. Lindsey<sup>\*1</sup>

<sup>1</sup>Department of Chemistry, North Carolina State University, Raleigh, NC

<sup>2</sup>Department of Chemistry, Washington University, St. Louis, MO

<sup>3</sup>Department of Chemistry, University of California Riverside, Riverside, CA

Received 25 June 2007; accepted 12 July 2007; DOI: 10.1111/j.1751-1097.2007.00195.x

### ABSTRACT

The ability to tailor synthetic porphyrin, chlorin and bacteriochlorin molecules holds promise for diverse studies in artificial photosynthesis. Toward this goal, the synthesis and photophysical characterization of five tetrapyrrole compounds is described. Each compound bears a surface attachment group. One set contains three meso-substituted porphyrins that differ only in the nature of a surface-binding tether—*isophthalic acid*, *ethynylisophthalic acid* or *cyanoacrylic acid*. The other set includes a porphyrin, chlorin and bacteriochlorin each of which bears an ethynylisophthalic acid tether. The ester derivative of each compound was prepared for solution photophysical characterization studies. The photophysical studies include determination (in toluene or acetonitrile) of the electronic absorption and fluorescence spectra, fluorescence yield and lifetime of the lowest excited singlet state. The excited-state lifetimes range from 1 to 5.6 ns for the five compounds. The radiative rate constant for the excited-state decay was estimated from the photophysical data (fluorescence yield and excited-state lifetime) and from Strickler–Berg analysis of the absorption and fluorescence spectra. The synthesis and characterization of the tetrapyrrole compounds underpin their use as sensitizers in molecular-based solar cells.

### INTRODUCTION

A chief objective of artificial photosynthesis is to learn how to design and prepare synthetic constructs that duplicate the various steps of natural photosynthetic systems. Toward that goal, a vast amount of work has been carried out with synthetic porphyrins as surrogates for the chlorophylls and bacteriochlorophylls of photosynthetic systems. The rationale for use of porphyrins rather than chlorins or bacteriochlorins stems from the close structural resemblance of the macrocycles and the more facile synthesis of porphyrins *versus* chlorins or bacteriochlorins. Porphyrins, chlorins and bacteriochlorins share a common macrocyclic skeleton containing 20 carbons and four inner nitrogens yet differ in the degree of saturation of the  $\pi$  system. The porphyrin is fully unsaturated, the chlorin is a dihydroporphyrin wherein one  $\beta,\beta'$ -bond is saturated and

the bacteriochlorin is a tetrahydroporphyrin wherein a  $\beta,\beta'$ -bond in each of two rings positioned *trans* to each other is saturated. The progressive saturation of the macrocycle (porphyrin  $\rightarrow$  chlorin  $\rightarrow$  bacteriochlorin) leads to an increased wavelength and intensity of the lowest-energy absorption band. In particular, porphyrins absorb relatively weakly in the red region; chlorins absorb strongly in the red region; bacteriochlorins absorb very strongly in the near-infrared region (1). A comparison of the absorption spectra (2) of these three types of macrocycles is shown in Fig. 1. Thus, the use of porphyrins as surrogates for chlorins and bacteriochlorins achieves synthetic expediency yet sacrifices solar coverage.

The use of porphyrins in lieu of chlorins or bacteriochlorins also leaves unexamined key attributes of the latter molecules that differ from porphyrins. Such features include (i) less positive oxidation potential (*i.e.* greater ease of oxidation), (ii) more negative reduction potential (*i.e.* more difficult reduction), (iii) lower energy first singlet excited state and (iv) lower symmetry ( $C_{2v}$  or  $D_{2h}$  *versus*  $D_{4h}$  for metalloporphyrins), and hence an excited state that exhibits features of a linear oscillator rather than a planar oscillator. Thus, there are multiple rationales, in addition to the biomimetic imperative and the overt reason of increased spectral coverage, to pursue the examination of chlorins and bacteriochlorins in artificial photosynthetic systems (3).

Examination of the photoreactivity of chlorins and bacteriochlorins in artificial solar-conversion constructs requires the ability to organize the molecules in well-defined architectures. In this regard, the syntheses of these classes of non-saturated macrocycles have presented obstacles. Three approaches generally have been employed for the synthesis of model (bacterio)chlorins. (i) *Reduction or derivatization of porphyrins*: This approach is the simplest yet least versatile, typically affording mixtures of isomers with porphyrins that bear distinct patterns of substituents (4,5). (ii) *Semisynthesis*: The chemical modification of naturally occurring (bacterio)chlorophylls takes advantage of ample quantities of naturally available starting materials. Although inherently limited by the presence of nearly a full complement of substituents arrayed about the perimeter of the macrocycle, numerous studies have exploited this approach to probe the role of diverse substituents about the chlorin macrocycle (6–15). A major challenge toward semisynthesis of bacteriochlorophylls resides in the intrinsic lability of the

\*Corresponding author emails: holten@wustl.edu (Dewey Holten); dbocian@ucr.edu (David Bocian); jlindsey@ncsu.edu (Jonathan S. Lindsey)

© 2007 The Authors. Journal Compilation. The American Society of Photobiology 0031-8655/07

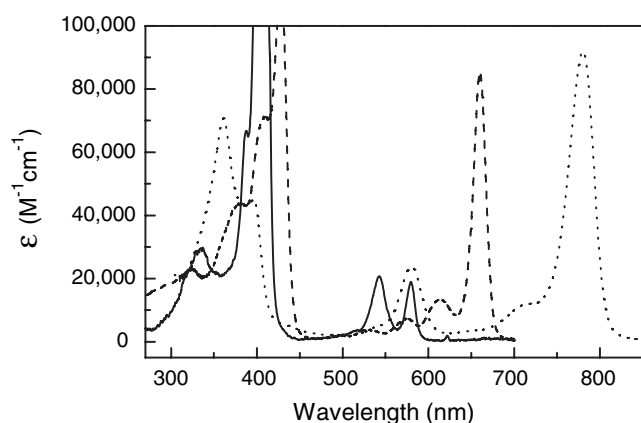


**Figure 1.** Absorption spectra for a porphyrin (solid line), a chlorin (dashed line) and a bacteriochlorin (dotted line). All three compounds are magnesium chelates: magnesium octaethylporphyrin, chlorophyll *a* and bacteriochlorophyll *a*, respectively. The peak violet-blue (Soret) region molar absorption coefficients are  $408 \text{ mM}^{-1} \text{ cm}^{-1}$  (408 nm),  $112 \text{ mM}^{-1} \text{ cm}^{-1}$  (428 nm) and  $71 \text{ mM}^{-1} \text{ cm}^{-1}$  (361 nm), respectively (2).

molecules (16–22). (iii) *De novo synthesis*: This approach, which we have pursued, entails the total synthesis of chlorins and bacteriochlorins from simple, commercially available precursors. In this approach, each target chlorin or bacteriochlorin is designed to contain a geminal dimethyl group in each reduced ring to prevent adventitious dehydrogenation (which ultimately would cause reversion to the porphyrin). The use of the geminal dimethyl group and the typical objective of a limited number of substituents make this approach far more accessible than the total synthesis of the naturally occurring (bacterio)chlorophylls. The core structures of the stable chlorin and bacteriochlorin are shown in Chart 1. The synthetic route to chlorins is quite versatile and has enabled introduction of substituents at each site at the perimeter of the macrocycle except position 7 (23–34). The synthetic route to bacteriochlorins has been developed quite recently. To date, substituents can be introduced at the 2, 12 and 15-positions (35,36). The *de novo* syntheses afford stable chlorins and bacteriochlorins, and enable the macrocycles to be tailored in a controlled manner without elaborate synthesis.

A long-term objective is to employ the stable synthetic chlorins and bacteriochlorins in a variety of fundamental studies in artificial photosynthesis. One attractive approach relies on the attachment of porphyrinic molecules to surfaces for studies of interfacial photoinduced electron-transfer reactions. In this regard, porphyrins bearing a wide variety of tethers have been synthesized for attachment to metal-oxide surfaces. The tethers include carboxylic acid (37), benzoic acid (38–41), vinylbenzoic acid (41,42), phenylphosphonic acid (43), vinylphenylphosphonic acid (41), benzylphosphonic acid (44),  $\alpha$ -cyanoacrylic acid (45,46), rhodanine (47), isophthalic acid (48), vinylisophthalic acid (42), ethynylbenzoic acid (49) and thiophenecarboxylic acid (50). Tethers that have been employed for attaching dyes (other than porphyrins) to metal-oxide surfaces include bidentate moieties such as isophthalic acid (42), cyanoacrylic acid (42,45,46) and alkenyl or alkynyl homologs thereof (49–57).

With synthetic access to chlorins and bacteriochlorins in hand, one objective was to prepare a set of tetrapyrrole compounds (porphyrin, chlorin and bacteriochlorin) bearing identical tethers for surface attachment. To this end, we have prepared a porphyrin (**ZnP-EI**), a chlorin (**ZnC-EI**) and a

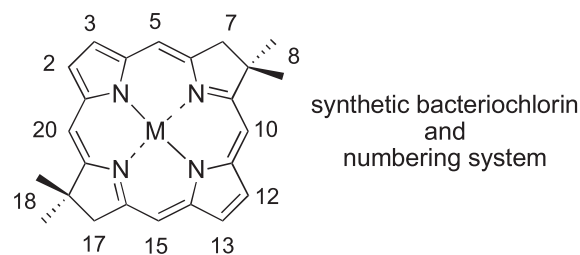
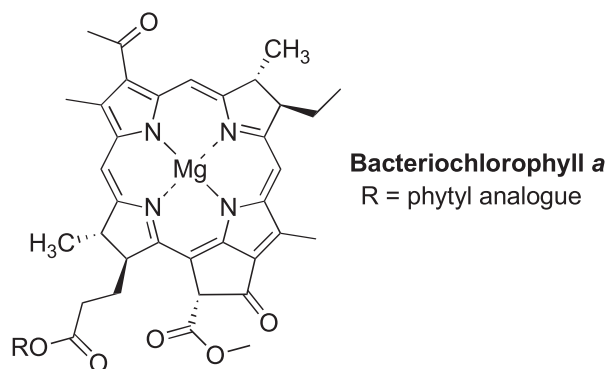
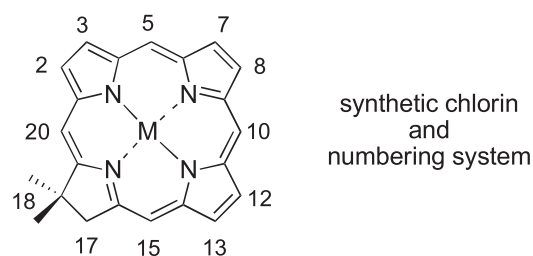
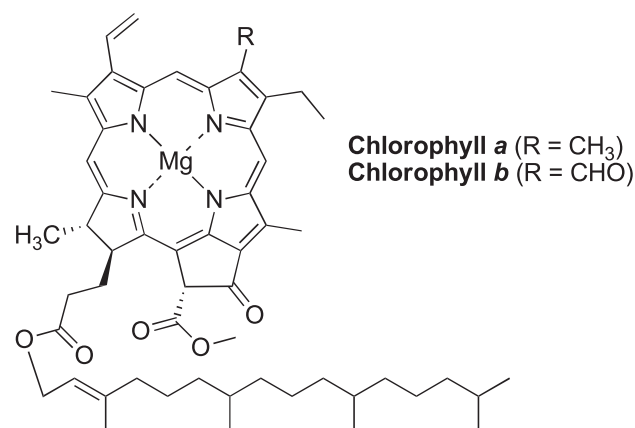


**Chart 1**

bacteriochlorin (**FbB-EI**) each bearing an ethynylisophthalic acid tether (Chart 2). The three compounds with identical tethers enables examination of the effects of increasing red-region and decreasing blue-region absorption, thermodynamic features and fundamental photophysical attributes as a function of increasing macrocycle saturation (porphyrin  $\rightarrow$  chlorin  $\rightarrow$  bacteriochlorin). We have also prepared two other *meso*-functionalized porphyrins bearing different tethers. The

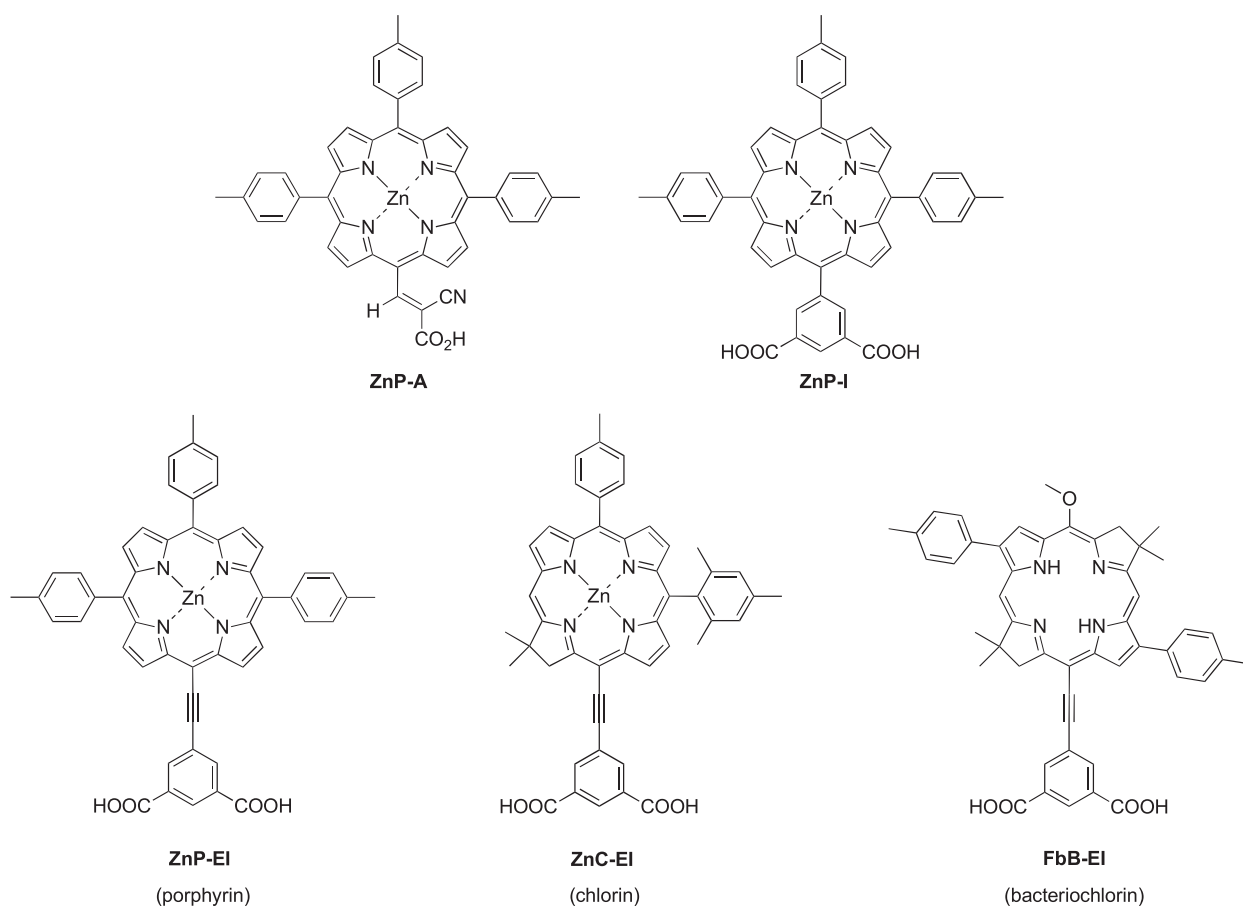


Chart 2

porphyrins are zinc chelates bearing a cyanoacrylic acid tether (**ZnP-A**) or an isophthalic acid tether (**ZnP-I**). The chlorin is also a zinc chelate whereas the bacteriochlorin lacks a metal (free base). A free base bacteriochlorin was examined rather than a zinc bacteriochlorin because effective synthetic methods for metalating bacteriochlorins are not yet available.

The synthesis of the five tetrapyrrole compounds shown in Chart 2 is described here, along with the photophysical characterization of the ester derivatives (**ZnP-A'**, **ZnP-I'**, **ZnP-EI'**, **ZnC-EI'**, **FbB-EI'**). The performance of the acid derivatives of the five compounds upon attachment to TiO<sub>2</sub> surfaces (in Grätzel-type solar cells) along with detailed analysis of the electronic (optical/redox) properties of the sensitizers in terms of the underlying molecular-orbital characteristics will be reported elsewhere (3).

## MATERIALS AND METHODS

**General methods.** <sup>1</sup>H NMR (400 MHz) and <sup>13</sup>C NMR (100 MHz) spectra were collected at room temperature in CDCl<sub>3</sub> unless noted otherwise. Absorption spectra were obtained at room temperature. The tetrapyrrole compounds were analyzed using laser desorption mass spectrometry (LD-MS) in the absence of a matrix (58). Fast atom bombardment mass spectrometry (FAB-MS) data are reported for the molecule ion or protonated molecule ion. Metalation of free base compounds was monitored using fluorescence spectroscopy. Melting points are uncorrected. All commercially available reagents were used as received. All palladium-coupling reactions were carried out using standard Schlenk-line techniques.

**Noncommercial compounds.** Compounds **1** (59), **2** (60), **3** (59), **4** (61), **5** (61), **Zn-5** (61), **11** (27) and **12** (36) were prepared by following literature procedures.

**Synthesis procedures.** *Dibutyl[5,10-dihydro-1,9-bis(4-methylbenzoyl)-5-(4-methylphenyl)dipyrinato]tin(IV)* (**2**): Following a reported procedure (60), a solution of EtMgBr (187 mL, 187 mmol, 1.0 M solution in tetrahydrofuran [THF]) was added slowly to a tap-water-cooled flask containing a solution of **1** (8.80 g, 37.5 mmol) in toluene (375 mL) under argon. The resulting mixture was stirred at room temperature for 30 min. A solution of *p*-toluoyl chloride (12.5 mL, 94.0 mmol) in toluene (94 mL) was added for 10 min, and the resulting solution was stirred for 30 min. The reaction mixture was poured into saturated aqueous NH<sub>4</sub>Cl (750 mL) and ethyl acetate (750 mL). The organic layer was washed (water, brine), dried (Na<sub>2</sub>SO<sub>4</sub>) and filtered. The filtrate was concentrated to dryness. The residue was treated with triethylamine (TEA, 15.7 mL, 112 mmol) and Bu<sub>2</sub>SnCl<sub>2</sub> (11.4 g, 37.5 mmol) in CH<sub>2</sub>Cl<sub>2</sub> (150 mL) at room temperature for 30 min. The mixture was filtered over a silica pad (CH<sub>2</sub>Cl<sub>2</sub>). The eluate was concentrated to dryness. The residue was dissolved in a minimum amount of diethyl ether. Methanol was added, yielding a precipitate, which upon filtration afforded a pale yellow solid (14.1 g, 54%). Characterization data (<sup>1</sup>H NMR, <sup>13</sup>C NMR and FAB-MS spectra) were consistent with those obtained from samples prepared previously (62).

**5,10,15-Tris(4-methylphenyl)porphyrin** (**4**): Following a reported procedure (60), a solution of **2** (5.30 g, 7.53 mmol) in dry THF/MeOH (288 mL, 10:1) was treated with NaBH<sub>4</sub> (5.70 g, 150 mmol, 20 equiv) in small portions with rapid stirring at room temperature. After 2 h, analysis by thin layer chromatography (TLC) indicated incomplete conversion of **2**. Therefore, an additional amount of NaBH<sub>4</sub> (5.70 g) was added, and the reaction mixture was stirred for 2 h. The reaction mixture was quenched by slow addition of saturated aqueous NH<sub>4</sub>Cl. The reaction mixture was extracted with CH<sub>2</sub>Cl<sub>2</sub>. The organic layer

was separated, dried ( $K_2CO_3$ ) and concentrated to afford **2-diol** as a yellow foam-like solid. The freshly prepared **2-diol** was condensed with dipyrromethane **3** (1.09 g, 7.53 mmol) in  $CH_2Cl_2$  (2.99 L) under catalysis with  $Yb(OTf)_3$  (5.93 g, 11.3 mmol) at room temperature for 30 min (63,64). A sample of 2,3-dichloro-5,6-dicyano-1,4-benzoquinone (DDQ, 5.09 g) was added, and the reaction mixture was stirred for 1 h at room temperature. The reaction mixture was then neutralized with TEA (7.5 mL) and filtered through a pad of silica (eluted with  $CH_2Cl_2$ ). The first fraction was collected and concentrated. The resulting solid was subjected to column chromatography (silica, hexanes/ $CH_2Cl_2$  [1:1]) to afford a purple solid (1.60 g, 37%). Characterization data ( $^1H$  NMR, LD-MS, FAB-MS and UV-Vis spectra) were consistent with those obtained from samples prepared *via* earlier routes (61,62).

**5-Bromo-10,15,20-tris(4-methylphenyl)porphyrin (5)**: Following a reported procedure (61), a solution of **4** (1.00 g, 1.72 mmol) in  $CHCl_3$  (430 mL) was treated with *N*-bromosuccinimide (NBS, 306 mg, 1.72 mmol) and pyridine (1.70 mL) at 0°C for 30 min. Acetone (2 mL) was added. The reaction mixture was concentrated to dryness. The resulting solid was purified by column chromatography (silica, hexanes/ $CH_2Cl_2$  [1:1]) to give a purple solid (1.12 g, 99%). Characterization data ( $^1H$  NMR, LD-MS, FAB-MS, and UV-Vis spectra) were consistent with those obtained from samples prepared previously (61).

**Zn(II)-5-Bromo-10,15,20-tris(4-methylphenyl)porphyrin (Zn-5)**: A solution of  $Zn(OAc)_2 \cdot 2H_2O$  (3.33 g, 15.2 mmol) in methanol (35 mL) was added to a solution of **5** (1.00 g, 1.52 mmol) in  $CHCl_3$  (140 mL) with stirring at room temperature. After 16 h, the reaction mixture was concentrated, whereupon  $CH_2Cl_2$  (50 mL) was added. The organic layer was washed (saturated aqueous  $NaHCO_3$ ,  $H_2O$ ), dried ( $Na_2SO_4$ ) and concentrated. The resulting solid was purified by column chromatography (silica, hexanes/ $CH_2Cl_2$  [1:1]) to afford a purple solid (0.93 g, 85%). Characterization data ( $^1H$  NMR, LD-MS, FAB-MS and UV-Vis spectra) were consistent with those obtained from samples prepared previously (61).

**5-[Bis(ethoxycarbonyl)methyl]-10,15,20-tris(4-methylphenyl)porphyrin (6)**: Diethyl malonate (97.4 mg, 0.608 mmol) was added dropwise to  $NaH$  (24.3 mg, 0.608 mmol, 60% dispersion in mineral oil) in dimethylsulfoxide (DMSO, 10.0 mL) at 100°C. The mixture was stirred until all solids had dissolved (~30 min), and then allowed to cool to room temperature. Bromoporphyrin **5** (100 mg, 0.152 mmol) was added all at once, and the mixture was heated at 100°C for 20 h under argon. The reaction mixture was allowed to cool to room temperature and then diluted with ethyl acetate (50 mL). The organic layer was washed with  $H_2O$ , dried ( $Na_2SO_4$ ) and concentrated. The resulting residue was purified by column chromatography (silica, hexanes then hexanes/ $CH_2Cl_2$  [1:1.5]) to give a purple solid (90.1 mg, 80%):  $^1H$  NMR  $\delta$  -2.72 (br, 2H), 1.15 (t,  $J = 7.2$  Hz, 6H), 2.69 (s, 3H), 2.70 (s, 6H), 4.28–4.32 (m, 4H), 7.33 (s, 1H), 7.54–7.57 (m, 6H), 8.06–8.09 (m, 6H), 8.80 (d,  $J = 4.8$  Hz, 2H), 8.83 (d,  $J = 4.8$  Hz, 2H), 8.95 (d,  $J = 4.8$  Hz, 2H), 9.51 (d,  $J = 4.8$  Hz, 2H);  $^{13}C$  NMR  $\delta$  14.2, 21.7 (two overlapped resonances), 58.3, 62.4, 108.6, 120.5, 121.5, 127.5, 127.7, 134.6, 134.7, 137.6, 139.0, 139.5, 143.3, 170.3, resonances from the  $\alpha$ - and  $\beta$ -carbons of the porphyrin were not observed because of NH tautomerism; LD-MS obsd 738.1; FAB-MS obsd 739.3318, calcd 739.3284 ( $C_{48}H_{42}N_4O_4$ );  $\lambda_{abs}$  ( $CH_2Cl_2$ ) 419, 516, 551, 591 nm.

**5-Formyl-10,15,20-tris(4-methylphenyl)porphyrin (7)**: A mixture containing **6** (50.0 mg, 0.0676 mmol) in 6.0 mL of 20% aqueous HCl acid was refluxed for 24 h. The reaction mixture was allowed to cool to room temperature, and then diluted with ethyl acetate (80 mL). The organic layer was washed (saturated aqueous  $NaHCO_3$ ,  $H_2O$ ), dried ( $Na_2SO_4$ ) and concentrated. The resulting residue was purified (silica, hexanes then hexanes/ $CH_2Cl_2$  [1:2]) to afford a trace amount (~5% of the total) of a *meso*-methyl porphyrin followed by the title compound as a purple solid (32.1 mg, 78%):  $^1H$  NMR  $\delta$  -2.00 (br, 2H), 2.71 (s, 3H), 2.72 (s, 6H), 7.54–7.58 (m, 6H), 8.03–8.06 (m, 6H), 8.70 (d,  $J = 4.8$  Hz, 2H), 8.77 (d,  $J = 4.8$  Hz, 2H), 8.77 (d,  $J = 4.8$  Hz, 2H), 9.98 (d,  $J = 4.8$  Hz, 2H), 12.45 (s, 1H);  $^{13}C$  NMR (75 MHz)  $\delta$  21.7 (two overlapped resonances), 107.6, 123.1, 126.1, 127.7, 127.8, 134.4, 134.5, 138.0, 138.1, 138.4, 138.9, 195.0, resonances from the  $\alpha$ - and  $\beta$ -carbons of the porphyrin were not observed because of NH tautomerism; LD-MS obsd 608.3; FAB-MS obsd 609.2675, calcd 609.2654 ( $C_{42}H_{32}N_4O$ );  $\lambda_{abs}$  ( $CH_2Cl_2$ ) 426, 530, 571, 601 nm.

**Zn(II)-5-Formyl-10,15,20-tris(4-methylphenyl)porphyrin (Zn-7)**: A solution of  $Zn(OAc)_2 \cdot 2H_2O$  (173 mg, 0.787 mmol) in methanol (2 mL) was added to a solution of **7** (32.0 mg, 0.0525 mmol) in  $CHCl_3$  (8 mL) with stirring at room temperature. After 5 h, TLC analysis indicated that the reaction was complete with the appearance of a new, polar band (green). The reaction mixture was concentrated, whereupon ethyl acetate (50 mL) was added. The organic layer was washed (saturated aqueous  $NaHCO_3$ ,  $H_2O$ ), dried ( $Na_2SO_4$ ) and concentrated. The resulting solid was purified by column chromatography (hexanes then  $CH_2Cl_2$ /methanol [95:5]) to afford a green solid (33.5 mg, 95%):  $^1H$  NMR (THF- $d_6$ )  $\delta$  2.67 (s, 3H), 2.70 (s, 6H), 7.56–7.59 (m, 6H), 8.01–8.05 (m, 6H), 8.68 (d,  $J = 4.8$  Hz, 2H), 8.75 (d,  $J = 4.8$  Hz, 2H), 8.95 (d,  $J = 4.8$  Hz, 2H), 10.15 (d,  $J = 4.8$  Hz, 2H), 12.57 (s, 1H);  $^{13}C$  NMR (75 MHz, THF- $d_6$ )  $\delta$  21.7 (two overlapped resonances), 109.6, 124.1, 127.2, 128.1, 128.2, 130.3, 131.8, 133.1, 134.9, 135.1, 135.2, 138.2, 138.3, 141.0, 141.2, 150.2, 150.3, 152.7, 154.5, 195.8; LD-MS obsd 670.2; FAB-MS obsd 670.1710, calcd 670.1711 ( $C_{42}H_{30}N_4OZn$ );  $\lambda_{abs}$  ( $CH_2Cl_2$ ) 430, 564, 604 nm.

**Zn(II)-5-(2-Cyano-2-methoxycarbonylvinyl)-10,15,20-tris(4-methylphenyl)porphyrin (ZnP-A')**: A mixture of **Zn-7** (7.30 mg, 0.0108 mmol), methyl cyanoacetate (4.80  $\mu$ L, 0.0540 mmol) and piperidine (16.1  $\mu$ L, 0.108 mmol) in anhydrous methanol (2.0 mL) was refluxed under argon. After 6 h, the reaction mixture was concentrated under reduced pressure. The resulting solid was chromatographed (silica, hexanes then  $CH_2Cl_2$ ) to afford a green solid (6.20 mg, 76%):  $^1H$  NMR (300 MHz)  $\delta$  2.70 (s, 3H), 2.72 (s, 6H), 4.17 (s, 3H), 7.53–7.60 (m, 6H), 8.04–8.08 (m, 6H), 8.86 (d,  $J = 4.8$  Hz, 2H), 8.90 (d,  $J = 4.8$  Hz, 2H), 9.04 (d,  $J = 4.8$  Hz, 2H), 9.38 (d,  $J = 4.8$  Hz, 2H), 10.92 (s, 1H);  $^{13}C$  NMR (75 MHz)  $\delta$  21.7 (two overlapped resonances), 50.9, 111.6, 111.7, 113.3, 117.3, 123.5, 125.0, 127.3, 127.5, 129.2, 129.7, 131.1, 132.3, 132.7, 133.0, 134.5, 134.6, 137.7, 139.7, 150.5, 150.7, 151.2, 157.5, 169.3; LD-MS obsd 751.7; FAB-MS obsd 751.1946, calcd 751.1926 ( $C_{46}H_{33}N_5O_2Zn$ );  $\lambda_{abs}$  (toluene) 449, 565, 621 nm.

**Zn(II)-5-(2-Cyano-2-carboxyvinyl)-10,15,20-tris(4-methylphenyl)porphyrin (ZnP-A)**: Following a reported procedure (45), a mixture of **Zn-7** (23.0 mg, 0.0342 mmol), cyanoacetic acid (145 mg, 0.171 mmol) and piperidine (0.102 mL, 1.03 mmol) in anhydrous methanol (1.5 mL) was refluxed for 16 h under argon. While the solution was allowed to cool to room temperature,  $CH_2Cl_2$  (25 mL) and  $H_2O$  (50 mL) were added. The resulting solution was shaken vigorously, whereupon the aqueous layer was adjusted to pH ~2 with 2 M aqueous  $H_3PO_4$ . The organic layer was then separated and concentrated. The resulting solid was purified by column chromatography (silica, hexanes then  $CH_2Cl_2$ /methanol [85:15]) to give a green solid (20.0 mg, 79%):  $^1H$  NMR (DMSO- $d_6$ )  $\delta$  2.66 (s, 3H), 2.67 (s, 6H), 7.59–7.61 (m, 6H), 8.03–8.05 (m, 6H), 8.72 (d,  $J = 4.8$  Hz, 2H), 8.75 (d,  $J = 4.8$  Hz, 2H), 8.84 (d,  $J = 4.8$  Hz, 2H), 9.37 (d,  $J = 4.8$  Hz, 2H), 10.54 (s, 1H), 11.71 (br, 1H); LD-MS obsd 738.2, 693.3 ( $CO_2$  cleavage); ESI-MS obsd 737.0; FAB-MS obsd 737.1764, calcd 737.1769 ( $C_{45}H_{31}N_5O_2Zn$ );  $\lambda_{abs}$  (THF) 430, 565, 620 nm.

**Dimethyl-5-(4,4,5,5-tetramethyl-1,3,2-dioxaborolyl)isophthalate (8)**: A solution of dimethyl 5-iodoisophthalate (320 mg, 1.00 mmol), TEA (0.420 mL, 3.00 mmol) and 4,4,5,5-tetramethyl-1,3,2-dioxaborolane (0.220 mL, 1.50 mmol) was treated with [1,1'-bis(diphenylphosphino)ferrocene]dichloropalladium(II) [ $PdCl_2(dppf)$ ], 44.0 mg, 0.0600 mmol] in acetonitrile (4 mL). After being stirred for 5 h at 85°C under argon (on the Schlenk line), the mixture was allowed to cool to room temperature and then concentrated to dryness.  $Et_2O$  was added, and the mixture was filtered (to remove triethylammonium iodide). The filtrate was concentrated and treated with hexanes (30 mL). The resulting mixture was filtered. The filtrate was concentrated and chromatographed (silica,  $CHCl_3$  containing 1% TEA) to afford a white solid (160 mg, 50%): mp 134–135°C;  $^1H$  NMR  $\delta$  1.36 (s, 12H), 3.94 (s, 6H), 8.63 (d,  $J = 1.6$  Hz, 2H), 8.76 (t,  $J = 1.6$  Hz, 1H);  $^{13}C$  NMR  $\delta$  166.5, 140.1, 133.5, 130.3, 84.6, 52.5, 25.1; Anal. calcd for  $C_{16}H_{21}BO_6$ : C, 60.03; H, 6.661; Found: C, 60.24; H, 6.56.

**5-[3,5-Bis(methoxycarbonyl)phenyl]-10,15,20-tris(4-methylphenyl)porphyrin (FBP-I')**: Following a reported procedure (65), samples of **5** (50.0 mg, 0.0760 mmol), **8** (25.5 mg, 0.0760 mmol), anhydrous  $K_2CO_3$  (157 mg, 1.14 mmol) and  $Pd(PPh_3)_4$  (17.6 mg, 0.0152 mmol, 20 mol%) were weighed in a 25 mL Schlenk flask. The flask was pump-purged with argon three times. Toluene/*N,N*-dimethylformamide (DMF) (9.0 mL, 2:1) was added, and the mixture was heated to

95°C. TLC of the reaction mixture indicated incomplete consumption of the starting porphyrin after 6 h. Therefore, an additional amount of Pd(PPh<sub>3</sub>)<sub>4</sub> (17.6 mg) was added, and the reaction mixture was stirred for 12 h at 95°C. The solvent was removed. The residue was filtered through a pad of silica (CH<sub>2</sub>Cl<sub>2</sub>) followed by column chromatography of the resulting solid (silica, hexanes then hexanes/CH<sub>2</sub>Cl<sub>2</sub> [1:2]) to afford a purple solid (46.2 mg, 78%): <sup>1</sup>H NMR (THF-*d*<sub>8</sub>) δ -2.70 (br, 2H), 2.67 (s, 3H), 2.68 (s, 6H), 3.97 (s, 6H), 7.56–7.60 (m, 6H), 8.06–8.10 (m, 6H), 8.72 (d, *J* = 4.8 Hz, 2H), 8.83–8.85 (m, 4H), 8.86 (d, *J* = 4.8 Hz, 2H), 9.03–9.05 (m, 2H), 9.07–9.09 (m, 1H); <sup>13</sup>C NMR (75 MHz, THF-*d*<sub>8</sub>) δ 20.5, 21.7, 52.8, 117.0, 120.7, 121.0, 127.6 (two overlapped resonances), 129.4, 130.3, 131.3, 134.7 (two overlapped resonances), 137.7, 138.7, 139.2, 139.3, 143.4, 166.7, resonances from the α- and β-carbons of the porphyrin were not observed because of NH tautomerism; LD-MS obsd 772.6; FAB-MS obsd 772.3017, calcd 772.3050 (C<sub>51</sub>H<sub>40</sub>N<sub>4</sub>O<sub>4</sub>Zn); λ<sub>abs</sub> (CH<sub>2</sub>Cl<sub>2</sub>) 419, 515, 549, 593 nm.

*Zn(II)-5-[3,5-Bis(methoxycarbonyl)phenyl]-10,15,20-tris(4-methylphenyl)porphyrin (ZnP-I'*): A solution of Zn(OAc)<sub>2</sub>·2H<sub>2</sub>O (196 mg, 0.892 mmol) in methanol (2.0 mL) was added to a solution of **FbP-I'** (46.0 mg, 0.0595 mmol) in CHCl<sub>3</sub> (8.0 mL) with stirring at room temperature. After 16 h, the reaction mixture was concentrated and filtered through a pad of silica (hexanes then CH<sub>2</sub>Cl<sub>2</sub>) to afford a purple solid (45.8 mg, 92%): <sup>1</sup>H NMR (THF-*d*<sub>8</sub>) δ 2.67 (s, 3H + s, 6H), 3.96 (s, 6H), 7.54–7.58 (m, 6H), 8.04–8.09 (m, 6H), 8.72 (d, *J* = 4.8 Hz, 2H), 8.84–8.86 (m, 4H), 8.88 (d, *J* = 4.8 Hz, 2H), 9.02–9.04 (m, 2H), 9.06–9.08 (m, 1H); <sup>13</sup>C NMR (75 MHz, THF-*d*<sub>8</sub>) δ 21.6 (two overlapped resonances), 52.6, 118.1, 121.7, 122.0, 127.5 (two overlapped resonances), 129.4, 130.1, 131.3, 132.3, 132.4, 132.7, 134.6 (two overlapped resonances), 137.4, 138.5, 140.0, 140.1, 144.1, 144.2, 149.9, 150.7, 150.8, 150.9, 166.7; LD-MS obsd 836.4; FAB-MS obsd 834.2192, calcd 834.2185 (C<sub>51</sub>H<sub>38</sub>N<sub>4</sub>O<sub>4</sub>Zn); λ<sub>abs</sub> (THF) 426, 519, 557, 597 nm.

*Zn(II)-5-(3,5-Dicarboxyphenyl)-10,15,20-tris(4-methylphenyl)porphyrin (ZnP-I)*: Following a reported procedure (45), a solution of NaOH (53.6 mg, 1.34 mmol, 20 equiv per CO<sub>2</sub>Me) in H<sub>2</sub>O (0.40 mL) and methanol (1.0 mL) was added to a refluxing solution of porphyrin **ZnP-I'** (28.0 mg, 0.0335 mmol) in THF (2.0 mL) and methanol (1.0 mL) under argon. After 2 h, TLC analysis indicated that all of **ZnP-I'** had been consumed. After the mixture cooled to room temperature, the mixture was concentrated to remove the THF and methanol. The resulting mixture was diluted with H<sub>2</sub>O (5.0 mL), and the mixture was adjusted to pH ~2 using 2 M aqueous H<sub>3</sub>PO<sub>4</sub>. The resulting precipitate was isolated by centrifugation and filtration to give a purple powder (26.4 mg, 98%): <sup>1</sup>H NMR (THF-*d*<sub>8</sub>) δ 2.68 (s, 3H + s, 6H), 7.53–7.57 (m, 6H), 8.06–8.09 (m, 6H), 8.75 (d, *J* = 4.8 Hz, 2H), 8.85–8.87 (m, 4H), 8.87 (d, *J* = 4.8 Hz, 2H), 9.02–9.04 (m, 2H), 9.08–9.10 (m, 1H), resonances from the COOH of the porphyrin were not observed; <sup>13</sup>C NMR (THF-*d*<sub>8</sub>) δ 21.7 (two overlapped resonances), 119.0, 121.4, 121.8, 128.0, 128.4, 130.8, 131.1, 132.3, 132.4, 132.8, 135.3, 135.4, 137.8, 138.5, 139.4, 140.3, 141.6, 143.9, 145.2, 150.7, 151.3 (two overlapped resonances), 151.4, 167.7; LD-MS obsd 806.1; FAB-MS obsd 806.1806, calcd 806.1872 (C<sub>51</sub>H<sub>34</sub>N<sub>4</sub>O<sub>4</sub>Zn); λ<sub>abs</sub> (THF) 425, 520, 557, 597 nm.

*Zn(II)-5-[2-(3,5-Bis(methoxycarbonyl)phenyl)ethynyl]-10,15,20-tris(4-methylphenyl)porphyrin (ZnP-EI')*: Following a reported procedure for Sonogashira coupling with arylporphyrins (61,66,67), samples of **Zn-5** (70.0 mg, 0.0968 mmol) and dimethyl 5-ethynylisophthalate (25.3 mg, 0.116 mmol) were coupled using tris(dibenzylideneacetone)dipalladium(0) [Pd<sub>2</sub>(dba)<sub>3</sub>, 53.2 mg, 0.0580 mmol] and tri-*o*-tolylphosphine [P(*o*-tol)<sub>3</sub>, 133 mg, 0.435 mmol] in toluene/TEA (5:1, 36 mL) at 50°C under argon. After 16 h, the reaction mixture was concentrated under reduced pressure. The resulting residue was chromatographed (silica, hexanes then CH<sub>2</sub>Cl<sub>2</sub>/methanol [95:5]) to afford a greenish purple solid (74.0 mg, 89%): <sup>1</sup>H NMR (THF-*d*<sub>8</sub>) δ 2.67 (s, 3H), 2.70 (s, 6H), 4.02 (s, 6H), 7.54–7.59 (m, 6H), 8.03–8.09 (m, 6H), 8.69–8.71 (m, 1H), 8.77–8.78 (m, 4H), 8.82–8.85 (m, 2H), 8.95 (d, *J* = 4.8 Hz, 2H), 9.80 (d, *J* = 4.8 Hz, 2H); <sup>13</sup>C NMR (75 MHz, THF-*d*<sub>8</sub>) δ 21.7 (two overlapped resonances), 52.8, 93.6, 95.7, 122.1, 122.8, 123.4, 125.5, 127.3, 127.4, 130.4, 130.7, 131.3, 131.7, 132.2, 133.1, 134.5, 134.6, 134.9, 136.4, 137.2, 140.0, 140.2, 150.0, 150.9 (two overlapped resonances), 152.4, 166.0; LD-MS obsd 860.6; FAB-MS obsd 858.2218, calcd 858.2185 (C<sub>53</sub>H<sub>38</sub>N<sub>4</sub>O<sub>4</sub>Zn); λ<sub>abs</sub> (THF) 441, 531, 572, 623 nm.

*Zn(II)-5-[2-(3,5-Dicarboxyphenyl)ethynyl]-10,15,20-tris(4-methylphenyl)porphyrin (ZnP-EI)*: Following a reported procedure (45), a solution of NaOH (96.7 mg, 20 equiv per CO<sub>2</sub>Me, 2.42 mmol) in H<sub>2</sub>O (650 μL) and methanol (1.6 mL) was added to a refluxing solution of porphyrin **ZnP-EI'** (52.0 mg, 0.0604 mmol) in THF (3.2 mL) and methanol (1.6 mL) under argon. After 2 h, TLC analysis indicated that all of **ZnP-EI'** had been consumed. The solution was allowed to cool to room temperature, whereupon CH<sub>2</sub>Cl<sub>2</sub> (30 mL), H<sub>2</sub>O (60 mL) and 2 M aqueous H<sub>3</sub>PO<sub>4</sub> were added. The solution was shaken vigorously in a separatory funnel (pH ~2.0). The organic layer, which contained the porphyrin, was isolated. Acetone (30 mL) was added to the organic layer, and the solution was concentrated to a volume of ~5 mL. The product was precipitated by the addition of H<sub>2</sub>O. The resulting mixture was centrifuged and then filtered to give a greenish purple powder (46.0 mg, 91%): <sup>1</sup>H NMR (DMSO-*d*<sub>6</sub>) δ 2.66 (s, 3H), 2.68 (s, 6H), 7.58–7.64 (m, 6H), 8.01–8.07 (m, 6H), 8.57–8.58 (m, 1H), 8.70 (d, *J* = 4.8 Hz, 2H), 8.72 (d, *J* = 4.8 Hz, 2H), 8.79–8.80 (m, 2H), 8.89 (d, *J* = 4.8 Hz, 2H), 9.81 (d, *J* = 4.8 Hz, 2H), 13.70 (br, 2H); LD-MS obsd 829.7; FAB-MS obsd 830.1846, calcd 830.1872 (C<sub>51</sub>H<sub>34</sub>N<sub>4</sub>O<sub>4</sub>Zn); λ<sub>abs</sub> (THF) 440, 532, 573, 622 nm.

*5-Ethynylisophthalic acid (9)*: A solution of NaOH (1.03 g, 25.7 mmol, 20 equiv per CO<sub>2</sub>Me) in H<sub>2</sub>O (2.0 mL) and methanol (5.0 mL) was added to a refluxing solution of dimethyl 5-ethynylisophthalate (140 mg, 0.642 mmol) in THF (10 mL) and methanol (5.0 mL) under argon. After 2 h, TLC analysis indicated that all of the dimethyl 5-ethynylisophthalate had been consumed. After the mixture cooled to room temperature, the mixture was concentrated in vacuum to remove the THF and methanol. The resulting mixture was diluted with H<sub>2</sub>O (5.0 mL), and the mixture was adjusted to pH ~1 using aqueous 10% HCl. The resulting precipitate was isolated by centrifugation and filtration. The filtered material was washed with H<sub>2</sub>O to give a white powder (122 mg, 100%): mp 104–106°C [lit. mp 106.2°C (68)]; <sup>1</sup>H NMR (DMSO-*d*<sub>6</sub>) δ 4.46 (s, 1H), 8.13–8.15 (m, 2H), 8.43–8.44 (m, 1H), 13.56 (br, 2H); <sup>13</sup>C NMR (DMSO-*d*<sub>6</sub>) δ 81.5, 82.8, 123, 130, 132, 136, 166; Anal. calcd for C<sub>10</sub>H<sub>6</sub>O<sub>4</sub>: C, 63.16; H, 3.18. Found: C, 63.34; H, 3.42.

*1,3-Bis[2-(trimethylsilyl)ethoxycarbonyl]-5-ethynylbenzene (10)*: Following a general procedure (69), samples of **9** (177 mg, 0.931 mmol) and 2-(trimethylsilyl)ethanol (226 mg, 1.91 mmol) were dissolved in 5.0 mL of DMF. A sample of *N,N*-dicyclohexylcarbodiimide (DCC, 394 mg, 1.91 mmol) was added followed by 4-dimethylaminopyridine (23.0 mg, 0.186 mmol). A voluminous white precipitate formed immediately. After 14 h, ethyl acetate was added, and the mixture was filtered. The filtrate was concentrated and then treated with ethyl acetate. The resulting solution was washed with 5% NaHCO<sub>3</sub> and dried over Na<sub>2</sub>SO<sub>4</sub>. The solvent was removed under reduced pressure. The resulting residue was purified by column chromatography (silica, hexanes/ethyl acetate [95:5]) to give a white solid (125 mg, 34%): mp 51–52°C; <sup>1</sup>H NMR δ 0.09 (s, 18H), 1.13–1.18 (m, 4H), 3.16 (s, 1H), 4.42–4.47 (m, 4H), 8.28–8.30 (m, 2H), 8.50–8.63 (m, 1H); <sup>13</sup>C NMR δ -1.2, 17.7, 64.2, 79.1, 111.8, 123.2, 130.7, 131.7, 137.1, 150.0; Anal. calcd for C<sub>20</sub>H<sub>30</sub>O<sub>4</sub>Si<sub>2</sub>: C, 61.50; H, 7.74. Found: C, 61.64; H, 7.85.

*17,18-Dihydro-10-mesityl-15-[2-(3,5-bis(2-(trimethylsilyl)ethoxycarbonyl)phenyl)ethynyl]-18,18-dimethyl-5-(4-methylphenyl)porphyrin (FbC-EI')*: Following a general procedure for Sonogashira coupling (61,66,67), 15-bromochlorin **11** (75.3 mg, 120 μmol) and **10** (58.6 mg, 150 μmol) were coupled using Pd<sub>2</sub>(dba)<sub>3</sub> (16.5 mg, 18.0 μmol) and P(*o*-tol)<sub>3</sub> (43.7 mg, 144 μmol) in toluene/TEA (5:1, 48 mL) in a Schlenk flask at 60°C under argon. After 5 h, Pd<sub>2</sub>(dba)<sub>3</sub> (16.5 mg, 18.0 μmol) and P(*o*-tol)<sub>3</sub> (43.7 mg, 144 μmol) were added to the reaction mixture. After 12 h, the mixture was concentrated under reduced pressure. The residue was chromatographed (silica, hexanes then hexanes/CH<sub>2</sub>Cl<sub>2</sub> [1:1]) to afford a reddish purple solid (44.0 mg, 39%): <sup>1</sup>H NMR δ -1.05 (br, 1H), -0.91 (br, 1H), 0.16 (s, 18H), 1.25 (t, *J* = 8.5 Hz, 4H), 1.86 (s, 6H), 2.07 (s, 6H), 2.60 (s, 3H), 2.66 (s, 3H), 4.55 (t, *J* = 8.5 Hz, 4H), 4.77 (s, 2H), 7.23 (s, 2H), 7.48–7.51 (m, 2H), 7.97–8.00 (m, 2H), 8.22–8.24 (m, 1H), 8.35–8.37 (m, 1H), 8.55–8.57 (m, 1H), 8.68–8.73 (m, 5H), 8.75 (s, 1H), 9.16–9.18 (m, 1H); LD-MS obsd 936.4; FAB-MS obsd 936.4459, calcd 936.4466 (C<sub>58</sub>H<sub>64</sub>N<sub>4</sub>O<sub>4</sub>Si<sub>2</sub>); λ<sub>abs</sub> (toluene) 425, 565, 660 nm.

*Zn(II)-17,18-Dihydro-10-mesityl-15-[2-(3,5-bis(2-(trimethylsilyl)ethoxycarbonyl)phenyl)ethynyl]-18,18-dimethyl-5-(4-methylphenyl)porphyrin (ZnC-EI')*: A solution of **FbC-EI'** (37.5 mg, 40.0 μmol) in

CH<sub>2</sub>Cl<sub>2</sub> (10 mL) was treated with a methanol solution (1 mL) containing Zn(OAc)<sub>2</sub>·2H<sub>2</sub>O (176 mg, 0.800 mmol) at room temperature for 17 h. The reaction mixture was diluted with CH<sub>2</sub>Cl<sub>2</sub> (50 mL), washed with saturated aqueous NaHCO<sub>3</sub>, dried (Na<sub>2</sub>SO<sub>4</sub>) and filtered. The filtrate was concentrated to dryness. The residue was chromatographed (silica, hexanes then hexanes/CH<sub>2</sub>Cl<sub>2</sub> [1:2]) to afford a greenish purple solid (35.5 mg, 85%): <sup>1</sup>H NMR δ 0.16 (s, 18H), 1.24 (t, *J* = 8.5 Hz, 4H), 1.87 (s, 6H), 2.03 (s, 6H), 2.58 (s, 3H), 2.64 (s, 3H), 4.54 (t, *J* = 8.5 Hz, 4H), 4.67 (s, 2H), 7.20 (s, 2H), 7.44–7.48 (m, 2H), 7.90–7.93 (m, 2H), 8.10 (d, *J* = 4.3 Hz, 1H), 8.24 (d, *J* = 4.3 Hz, 1H), 8.41–8.43 (m, 2H), 8.51 (d, *J* = 4.3 Hz, 1H), 8.56 (d, *J* = 4.3 Hz, 1H), 8.61–8.63 (m, 2H), 8.65–8.67 (m, 1H), 9.03 (d, *J* = 4.3 Hz, 1H); <sup>13</sup>C NMR δ -1.1, 17.7, 21.3, 21.6, 21.7, 31.6, 44.6, 51.5, 64.2, 61.9, 92.8, 94.3, 96.1, 125.0, 125.8, 126.0, 126.4, 127.1, 127.7, 127.9, 129.5, 129.6, 131.8, 132.6, 133.6, 134.2, 136.1, 137.39, 137.51, 138.5, 138.9 (two overlapped resonances), 139.2, 145.8, 146.6, 147.5, 148.2, 155.00, 155.05, 164.3, 165.9, 171.6; LD-MS obsd 998.1; FAB-MS obsd 998.3563, calcd 998.3601 (C<sub>58</sub>H<sub>62</sub>N<sub>4</sub>O<sub>4</sub>Si<sub>2</sub>Zn); λ<sub>abs</sub> (toluene) 431, 624 nm.

**Zn(II)-15-[2-(3,5-Bis(2-(3,5-dicarboxyphenyl)ethynyl)-17,18-dihydro-10-mesityl-18,18-dimethyl-5-(4-methylphenyl)porphyrin (ZnC-EI):** A solution of ZnC-EI (20.0 mg, 20.0 μmol) in dry DMF (2 mL) was treated with KF (23.2 mg, 0.400 mmol) at 75°C for 12 h. The reaction mixture was concentrated to dryness. The resulting residue was chromatographed (silica, CH<sub>2</sub>Cl<sub>2</sub>/methanol [5:1]) to afford a fraction containing the mono-ester product (8.2 mg). Further elution with methanol gave a fraction containing the title compound, which was dried, dissolved in THF, filtered to remove silica gel and concentrated to dryness to afford the title compound (8.8 mg). A solution of the fraction containing the mono-ester in dry DMF (1.0 mL) was treated with KF (11.6 mg, 0.200 mmol), chromatographed and worked-up in the same manner to afford additional title compound (3.7 mg). Altogether, 12.5 mg (78% yield) of the title compound was obtained as a dark green solid: <sup>1</sup>H NMR (methanol-*d*<sub>4</sub>) δ 1.88 (s, 6H), 2.05 (s, 6H), 2.56 (s, 3H), 2.63 (s, 3H), 4.70 (s, 2H), 7.21 (s, 2H), 7.47–7.49 (m, 2H), 7.87–7.89 (m, 2H), 7.96 (d, *J* = 4.3 Hz, 1H), 8.10 (d, *J* = 4.3 Hz, 1H), 8.28 (d, *J* = 4.7 Hz, 1H), 8.41–8.43 (m, 2H), 8.47–8.50 (m, 3H), 8.62–8.63 (m, 1H), 9.04 (d, *J* = 4.7 Hz, 1H), a resonance from the COOH moieties of the chlorin was not observed because of D-H exchange; LD-MS obsd 798.2; FAB-MS obsd 798.2194, calcd 798.2185 (C<sub>48</sub>H<sub>38</sub>N<sub>4</sub>O<sub>4</sub>Zn); λ<sub>abs</sub> (methanol) 429, 600, 623 nm.

**5-Methoxy-8,8,18,18-tetramethyl-2,12-bis(4-methylphenyl)-15-[2-(3,5-bis(2-(trimethylsilyl)ethoxycarbonyl)phenyl)ethynyl]bacteriochlorin (FbB-EI):** Following a standard procedure (36,61,66,67), a mixture of **12** (26.0 mg, 0.0394 mmol), **10** (18.5 mg, 0.0473 mmol), Pd<sub>2</sub>(dba)<sub>3</sub> (5.41 mg, 0.00591 mmol) and P(*o*-tol)<sub>3</sub> (15.6 mg, 0.0512 mmol) was placed into a 50 mL Schlenk flask. Toluene/TEA (15.0 mL [5:1]) was added, and the reaction mixture was stirred at 50°C. After 6 h, Pd<sub>2</sub>(dba)<sub>3</sub> (5.41 mg, 0.00591 mmol) and P(*o*-tol)<sub>3</sub> (15.6 mg, 0.0512 mmol) were added. After 18 h, the mixture was concentrated to dryness. The resulting residue was purified by column chromatography (silica, hexanes then hexanes/CH<sub>2</sub>Cl<sub>2</sub> [3:7]) to afford a purple solid (24.0 mg, 63%): <sup>1</sup>H NMR (THF-*d*<sub>8</sub>) δ -1.54 (br, 1H), -1.25 (br, 1H), 0.16 (s, 18H), 1.25 (t, *J* = 8.5 Hz, 4H), 1.90 (s, 6H), 1.94 (s, 6H), 2.61 (s, 6H), 4.39 (s, 2H), 4.49 (s, 3H), 4.54 (t, *J* = 8.5 Hz, 4H), 4.69 (s, 2H), 7.57–7.60 (m, 4H), 8.10–8.15 (m, 4H), 8.66–8.70 (m, 3H), 8.83 (s, 1H), 8.86 (s, 1H), 8.96 (s, 1H), 9.20 (s, 1H); <sup>13</sup>C NMR (THF-*d*<sub>8</sub>) δ -1.1, 14.3, 17.7, 22.9, 31.0, 31.5, 45.5, 46.1, 47.5, 52.4, 64.2, 92.7, 93.5, 94.1, 96.4, 98.1, 116.9, 120.1, 125.6, 127.1, 129.0, 129.7, 130.00, 130.03, 130.5, 131.2, 131.3, 131.8, 133.6, 133.7, 133.9, 134.1, 134.9, 136.2, 137.1, 137.3, 137.7, 137.8, 154.0, 163.3, 165.8, 169.5, 170.6; LD-MS obsd 969.8; FAB-MS obsd 968.4772, calcd 968.4728 (C<sub>59</sub>H<sub>68</sub>N<sub>4</sub>O<sub>5</sub>Si<sub>2</sub>); λ<sub>abs</sub> (CH<sub>2</sub>Cl<sub>2</sub>) 387, 549, 758 nm.

**5-Methoxy-8,8,18,18-tetramethyl-2,12-bis(4-methylphenyl)-15-[2-(3,5-dicarboxyphenyl)ethynyl]bacteriochlorin (FbB-EI):** A solution of FbB-EI (19.0 mg, 0.0195 mmol) in 2.0 mL of THF was treated with tetrabutylammonium fluoride (TBAF, 0.195 mL, 10 equiv, 1 M THF) and stirred for 2 h at room temperature. The mixture was poured into CH<sub>2</sub>Cl<sub>2</sub>. The organic layer was extracted (5% NaHCO<sub>3</sub>, H<sub>2</sub>O), dried (Na<sub>2</sub>SO<sub>4</sub>) and concentrated. The resulting solid was chromatographed (silica, THF → ethanol) to give a purple solid (14.4 mg, 95%): <sup>1</sup>H NMR (methanol-*d*<sub>4</sub>) δ 1.90 (s, 6H), 1.93 (s, 6H), 2.61 (s, 6H), 4.39 (s, 2H), 4.49 (s, 3H), 4.69 (s, 2H), 7.58–7.63 (m, 4H), 8.06–8.12 (m, 4H), 8.53–8.55 (m, 2H), 8.70–8.71 (m, 1H), 8.77 (s, 1H), 8.80 (s, 1H), 8.90 (s,

1H), 9.15 (s, 1H), resonances from the NH and COOH protons of the bacteriochlorin were not observed because of D-H exchange; LD-MS obsd 769.0; FAB-MS obsd 769.3382, calcd 769.3390 (C<sub>49</sub>H<sub>44</sub>N<sub>4</sub>O<sub>5</sub>); λ<sub>abs</sub> (methanol) 387, 554, 755 nm.

**Optical spectroscopy.** Static absorption spectra (Cary 100) and fluorescence spectra and quantum yields (Spex Tau2; 5 nm bandpass) employed argon-purged solutions (1–10 μM for absorption and 0.3–1 μM for emission). Fluorescence yields were obtained using argon-purged samples with ZnTPP in toluene (Φ<sub>F</sub> = 0.030) (70) as a standard for ZnP-I' and ZnP-EI', and chlorophyll *a* in benzene (Φ<sub>F</sub> = 0.325) (71) as the standard for ZnC-EI' and FbB-EI'. Fluorescence lifetime studies employed 0.3–3 μM argon-purged solutions using a phase modulation technique (72). The absorption coefficients (ε) for the chlorin Zn(II)-17,18-dihydro-10-mesityl-18,18-dimethyl-5-(4-methylphenyl)porphyrin (ZnC-T<sup>5</sup>M<sup>10</sup>) and free base bacteriochlorin 5-methoxy-8,8,18,18-tetramethyl-2,12-bis(4-methylphenyl)bacteriochlorin (MeO-BC) in benzonitrile were determined from the known values in toluene (23, 35) as follows—the solvent was removed from three 3 mL aliquots of a stock solution of the compound (having measured absorbance spectrum and concentration) *via* use of a benchtop vacuum centrifuge. Then 3 mL of benzonitrile was added to each dried sample. The absorbance spectra were measured and the resulting three determinations of ε were averaged.

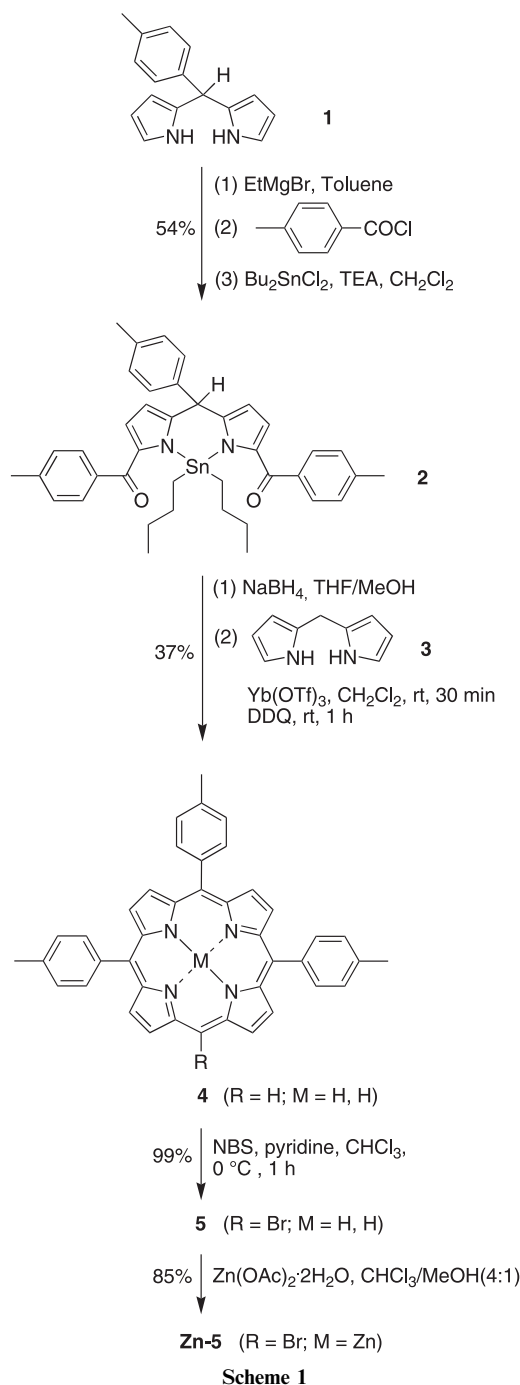
## RESULTS AND DISCUSSION

### Synthesis of tetrapyrrole compounds

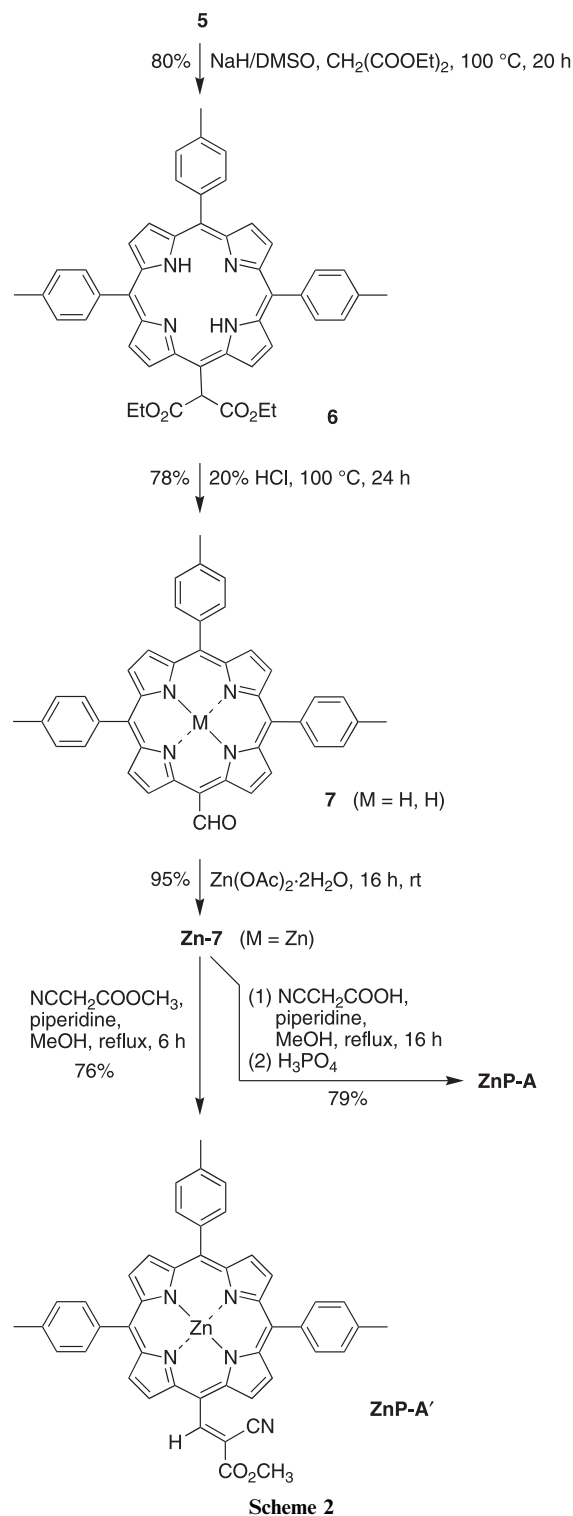
**Tethered porphyrins.** The synthetic approaches for the target porphyrins are as follows: (1) synthesis of the *meso*-acrylic acid derivative (ZnP-A) *via* a Knoevenagel condensation of a *meso*-formylporphyrin and cyanoacetic acid, (2) synthesis of the *meso*-isophthalic acid derivative (ZnP-I) *via* a Suzuki coupling reaction with a bromo-porphyrin followed by basic hydrolysis and (3) synthesis of the *meso*-ethynylisophthalic acid derivative (ZnP-EI) *via* a Sonogashira coupling reaction with a bromoporphyrin followed by basic hydrolysis. A key issue was to identify the suitability of the tether for surface attachment.

The target bromoporphyrin (Zn-5) for conversion to the three tethered porphyrins is a known compound (61). A refined synthesis at larger scale with improved procedures is described here and shown in Scheme 1. The diacylation of 5-(4-methylphenyl)dipyrrromethane (**1**) (59) with *p*-toluoyl chloride under the standard reaction conditions (60) followed by the treatment with Bu<sub>2</sub>SnCl<sub>2</sub> in CH<sub>2</sub>Cl<sub>2</sub> containing TEA afforded the corresponding tin complex **2** (60). The tin complex **2** was readily isolated by filtration through a pad of silica, whereupon the resulting solid was crystallized using diethyl ether and methanol. A large-scale synthesis of known porphyrin **4** (61,62) was carried out using the tin complex **2** and dipyrromethane **3** (59). Thus, the reduction of tin complex **2** (5.30 g) with NaBH<sub>4</sub> gave the putative dicarbinol **2-diol**. Condensation (63) of **2-diol** with dipyrromethane **3** (1.09 g) in the presence of improved acid catalysis conditions [Yb(OTf)<sub>3</sub> in CH<sub>2</sub>Cl<sub>2</sub> (64)] and oxidation with DDQ gave porphyrin **4** (1.60 g) in 37% yield. Bromination of **4** using 1 equiv of NBS afforded the bromoporphyrin **5** (61) in 99% yield. Treatment of **5** with Zn(OAc)<sub>2</sub>·2H<sub>2</sub>O in CHCl<sub>3</sub>/methanol (4:1) at room temperature gave Zn-5 in 85% yield.

The porphyrin bearing a cyanoacrylic acid (ZnP-A) tether is readily prepared by derivatization of a *meso*-formylporphyrin. A number of routes to *meso*-formylporphyrins have been devised (73). A new route for the synthesis of *meso*-formylporphyrins, which was discovered serendipitously, is shown in Scheme 2. Treatment of bromoporphyrin **5** with diethyl-



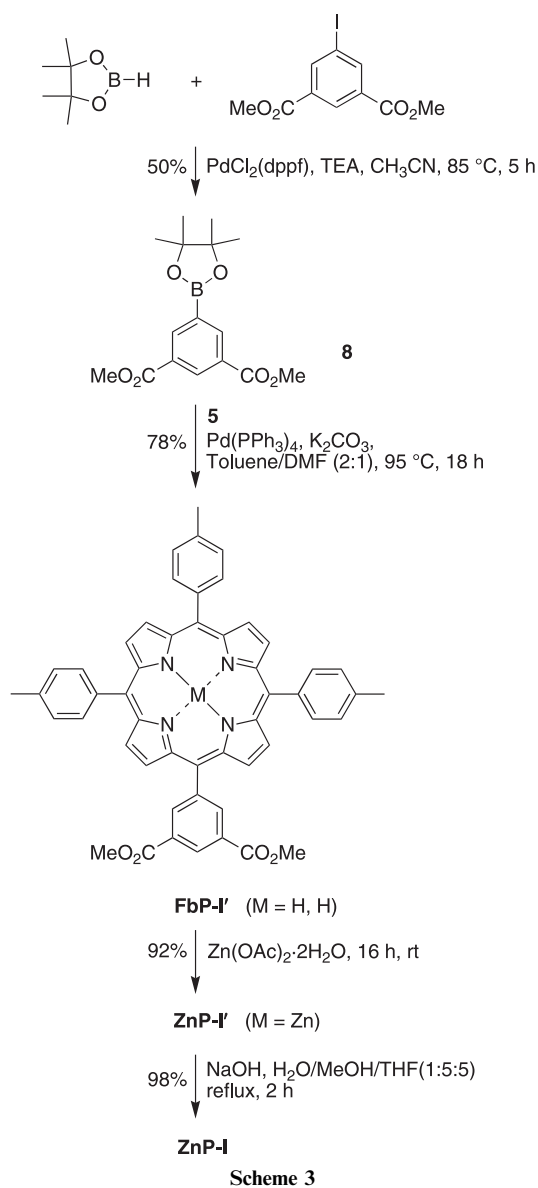
malonate in the presence of NaH/DMSO at 100°C for 20 h gave the diethylmalonate porphyrin **6** in 80% yield.  $^1\text{H}$  NMR spectroscopy, LD-MS and FAB-MS analyses established the structure of diethylmalonate porphyrin **6**. The characteristic methine proton in **6** shows a sharp singlet at  $\delta$  7.33 p.p.m. in the  $^1\text{H}$  NMR spectrum. Treatment of **6** with 20% aqueous HCl under reflux gave *meso*-formylporphyrin **7** in 78% yield. Although unexpected, this route of *meso*-bromination, substitution with diethyl malonate and *in situ* transformation to give the *meso*-formyl substituted free base porphyrin, provides a convenient alternative to traditional Vilsmeier formylation, which typically requires use of copper porphyrins. The reaction of **7** with Zn(OAc)2·2H2O gave **Zn-7** in 95% yield.



The synthesis of cyanoacrylic acid derivative **ZnP-A** is also shown in Scheme 2. The Knoevenagel condensation (45) of **Zn-7** with cyanoacetic acid in the presence of piperidine gave the crude piperidine salt, which upon subsequent treatment with phosphoric acid (pH  $\sim$  2) gave the carboxylic acid **ZnP-A** in good yield (79%) without demetalation. The Knoevenagel condensation was also applied to prepare the cyanoacrylic ester derivative **ZnP-A'** as a benchmark compound. Thus, treatment

of **Zn-7** with methyl cyanoacetate in the presence of piperidine afforded the cyanoacrylic ester derivative **ZnP-A'** in 76% yield.

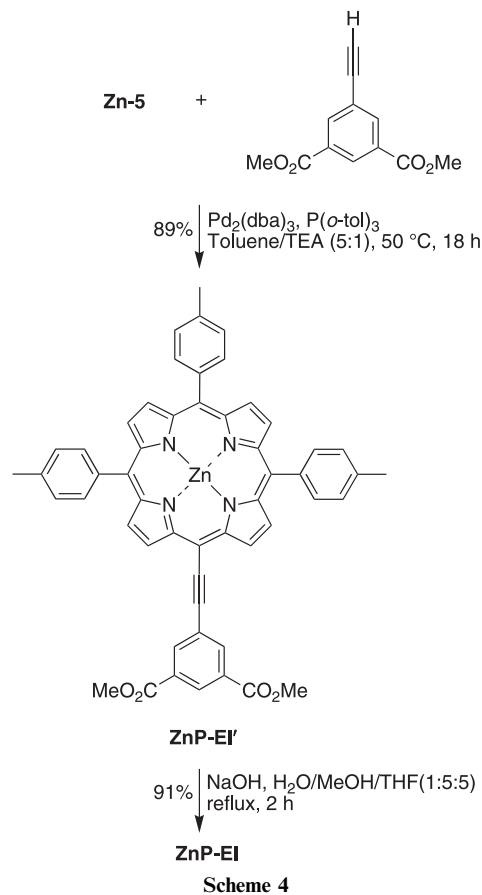
The synthesis of the porphyrin bearing an isophthalic acid (**ZnP-I**) tether was achieved through use of a Suzuki coupling reaction. The reported procedure for the synthesis of phenyl-linked porphyrin dyads and triads *via* the Suzuki coupling reaction was applied (65). The first step entailed utilization of a Suzuki coupling reagent with slight modifications of a literature method (74). Treatment of 4,4,5,5-tetramethyl-1,3,2-dioxaborolane with dimethyl 5-iodoisophthalate in dry CH<sub>3</sub>CN using PdCl<sub>2</sub>(dppf) and TEA at 85°C afforded the expected product **8** in 50% yield (Scheme 3). Equimolar amounts of bromoporphyrin **5** and **8** were coupled in toluene/DMF (2:1) using Pd(PPh<sub>3</sub>)<sub>4</sub> (20 mol%) and K<sub>2</sub>CO<sub>3</sub>. After 6 h at 95°C, TLC analysis of the reaction mixture indicated that some of the starting porphyrin remained unreacted. Therefore, an additional amount of Pd(PPh<sub>3</sub>)<sub>4</sub> (20 mol%) was added, and the reaction mixture was allowed to stir for 12 h at 95°C. The purification of the crude reaction

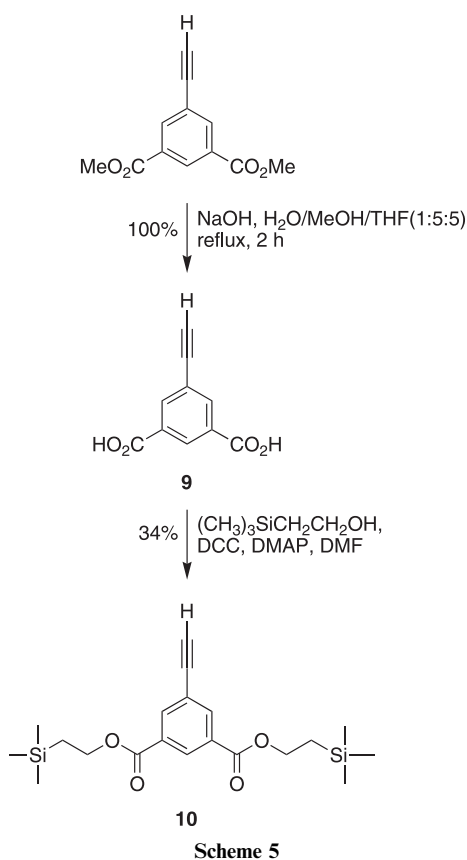


mixture by silica column chromatography afforded the porphyrin **FbP-I'** in 78% yield. Treatment of **FbP-I'** with Zn(OAc)<sub>2</sub>·2H<sub>2</sub>O in CHCl<sub>3</sub>/methanol (4:1) at room temperature gave **ZnP-I'** in 92% yield. The hydrolysis (45) of the ester in **ZnP-I'** using NaOH followed by acidic workup gave the isophthalic acid derivative **ZnP-I** in 98% yield.

The synthesis of a *meso*-ethynyl substituted porphyrin (**ZnP-EI**) was readily achieved using a copper-free Sonogashira coupling reaction (61). Thus, the reaction of **Zn-5** with dimethyl 5-ethynylisophthalate (75) in the presence of Pd<sub>2</sub>(dba)<sub>3</sub> and P(*o*-tol)<sub>3</sub> gave ethynyl-porphyrin **ZnP-EI'** in 89% yield (Scheme 4). The hydrolysis (45) of the ester in **ZnP-EI'** with sodium hydroxide (20 equiv per ester group) followed by acidic workup gave the ethynylisophthalic acid derivative **ZnP-EI** in good yield (91%).

*A tethered chlorin.* The route to a chlorin bearing a *meso*-ethynylisophthalic acid (**ZnC-EI**) tether was slightly modified from that employed for porphyrins. The chief difference was to use a protecting group that could be removed under mild conditions and thereby obtain the target containing free carboxylic acids at a late stage in the synthesis without affecting the macrocycle. To achieve this we chose the 2-(trimethylsilyl)ethyl moiety for the cleavable ester group. The synthesis of the corresponding linker **10** is shown in Scheme 5. Treatment of dimethyl 5-ethynylisophthalate with NaOH in THF/MeOH/H<sub>2</sub>O (5:5:1) at reflux for 2 h followed by acidic workup (10% aqueous HCl) gave the free ethynylisophthalic acid **9** in quantitative fashion. The ethynylisophthalic acid **9** is known; however, the prior method of

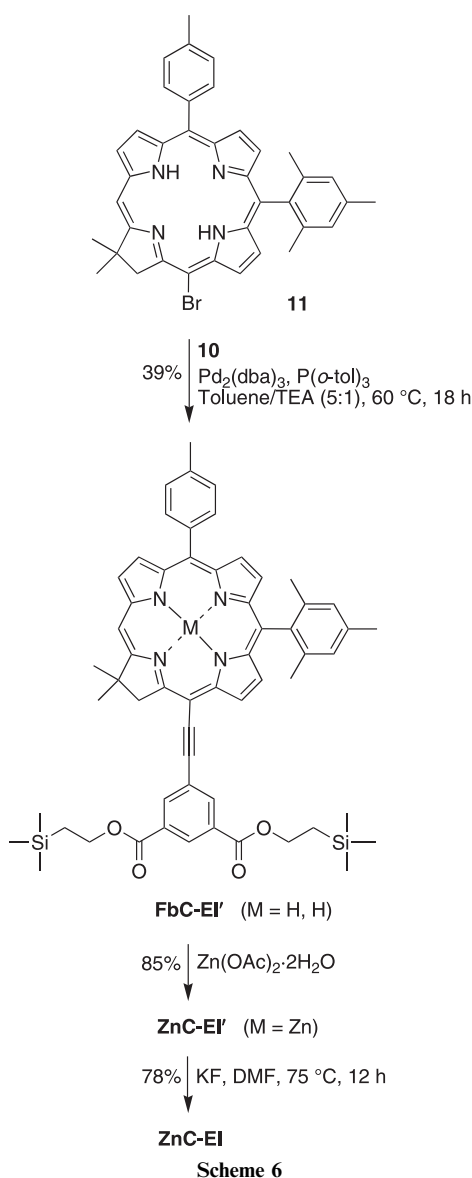




synthesis employed a different route (68). Following a literature procedure (69), linker **10** was obtained by reaction of **9** with 2-(trimethylsilyl)ethanol in the presence of DCC and DMAP in 34% yield.

Synthesis of the chlorin bearing the *meso*-ethynylisophthalic acid tether is shown in Scheme 6. The Sonogashira coupling of *meso*-substituted bromochlorin **11** (27) with **10** in the presence of  $\text{Pd}_2(\text{dba})_3$  and  $\text{P}(o\text{-tol})_3$  in toluene/TEA (5:1) afforded **FbC-EI'** in 39% yield. Treatment of **FbC-EI'** with  $\text{Zn}(\text{OAc})_2 \cdot 2\text{H}_2\text{O}$  in  $\text{CH}_2\text{Cl}_2$ /methanol (4:1) at room temperature gave **ZnC-EI'** in 85% yield. The deprotection of the 2-(trimethylsilyl)ethyl groups in **ZnC-EI'** was performed using KF to afford the free acid **ZnC-EI** in 78% yield.

*A tethered bacteriochlorin.* The route to a bacteriochlorin bearing a *meso*-ethynylisophthalic acid tether followed that of the chlorin synthesis. Stable synthetic bacteriochlorins have become available only recently (35). The bacteriochlorin bearing a 5-methoxy substituent (**MeO-BC**) was found to be readily brominated at the 15-position upon treatment with 1 equiv of NBS in THF at room temperature, thereby affording 15-bromobacteriochlorin **12** in 73% yield (36). The Sonogashira coupling of *meso*-bromobacteriochlorin **12** with **10** was carried out in the same manner as for the corresponding chlorin or porphyrin. Thus, the reaction of **12** and **10** in the presence of  $\text{Pd}_2(\text{dba})_3$  and  $\text{P}(o\text{-tol})_3$  in toluene/TEA (5:1) at 50°C afforded the bacteriochlorin conjugate **FbB-EI'** in 63% yield (Scheme 7). Deprotection (69) of the 2-(trimethylsilyl)ethyl groups in **FbB-EI'** was readily achieved using TBAF (5 equiv per ester group) to afford the corresponding free acid **FbB-EI**.

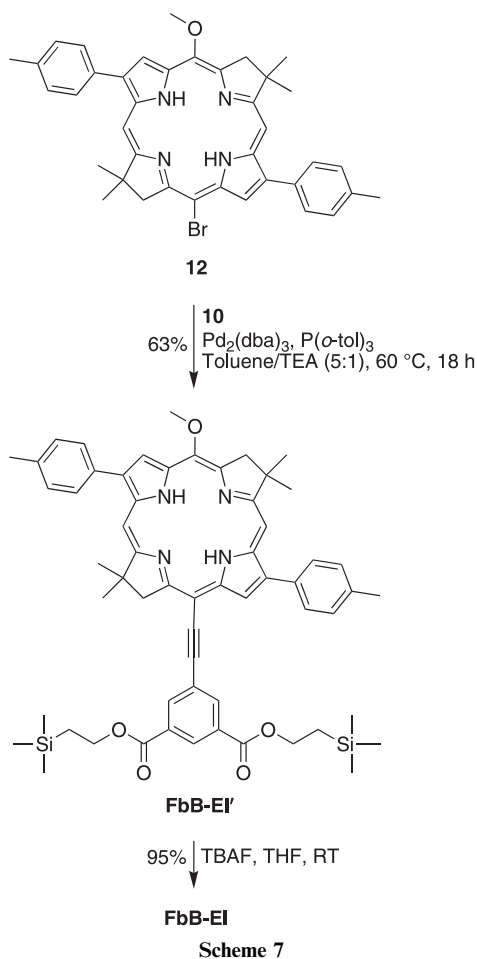


### Characterization of tetrapyrrole compounds

Each of the tetrapyrrole compounds for solar-cell studies bears a carboxylic acid for surface attachment (**ZnP-A**, **ZnP-I**, **ZnP-EI**, **ZnC-EI**, **FbB-EI**). Corresponding tetrapyrrole compounds bearing ester moieties were employed as benchmarks in solution photophysical characterization studies (**ZnP-A'**, **ZnP-I'**, **ZnP-EI'**, **ZnC-EI'**, **FbB-EI'**).

*Composition.* All porphyrins, chlorins and bacteriochlorins were characterized by  $^1\text{H}$  NMR spectroscopy, LD-MS and FAB-MS analyses. In addition,  $^{13}\text{C}$  NMR spectroscopy was performed for all compounds except those with insufficient solubility. In general, the porphyrinic compounds with insufficient solubility were those bearing free carboxylic acids (with the exception of **ZnP-I**). Additional characterization is described in the following sections.

The cyanoacrylic acid derivative **ZnP-A'** (or **ZnP-A**) is a trisubstituted alkene that in principle can exist in *cis* or *trans*



isomeric forms. <sup>1</sup>H NMR spectroscopy and chromatography of **ZnP-A'** (or **ZnP-A**) indicate the presence of only one isomer. It is essential to establish the configuration, given that the longest-wavelength absorption band of 2,2-disubstituted ethenyl-porphyrins (or hydroporphyrins) shifts depending on the *cis* or *trans* configuration. For example, Tamiaki and Kouraba reported that *trans*-isomers of the synthetic ethenyl-chlorins exhibited a longer-wavelength (up to 15 nm) transition than that of the corresponding *cis*-isomers (8). Only two cyanoacrylic acid-substituted porphyrins (or hydroporphyrins) have been reported to our knowledge, and each was reported to exist as the *trans*-isomer (8,45).

The configuration of **ZnP-A'** was assigned upon comparison of the chemical shift of the <sup>1</sup>H NMR spectrum for the corresponding resonances of vinyl protons of the following compounds (in CDCl<sub>3</sub>): (1) styrene, 6.72 p.p.m. (76); (2) (*E*)- and (*Z*)-3-phenyl-2-propenenitrile; *trans* 7.30 p.p.m., *cis* 7.03 p.p.m. (77); (3) *trans*- and *cis*-cinnamic acid; *trans* 7.81 p.p.m., *cis* 7.07 p.p.m. (78); (4) (*E*)-2-cyano-3-phenyl-2-propenoic acid, 8.32 p.p.m. (79); and (5) zinc(II)-5,15-divinyl-10,20-diphenyl porphyrin, 9.24 p.p.m. (80). On the basis of these data, the expected chemical shift of the resonance for the vinyl proton adjacent to the porphyrin meso carbon (5<sup>1</sup>-H) of **ZnP-A'** was calculated to be 10.64 p.p.m. for the *trans*-isomer and 10.17 p.p.m. for the *cis*-isomer, respectively. The observed resonance appeared at 10.92 p.p.m. Accordingly, the config-

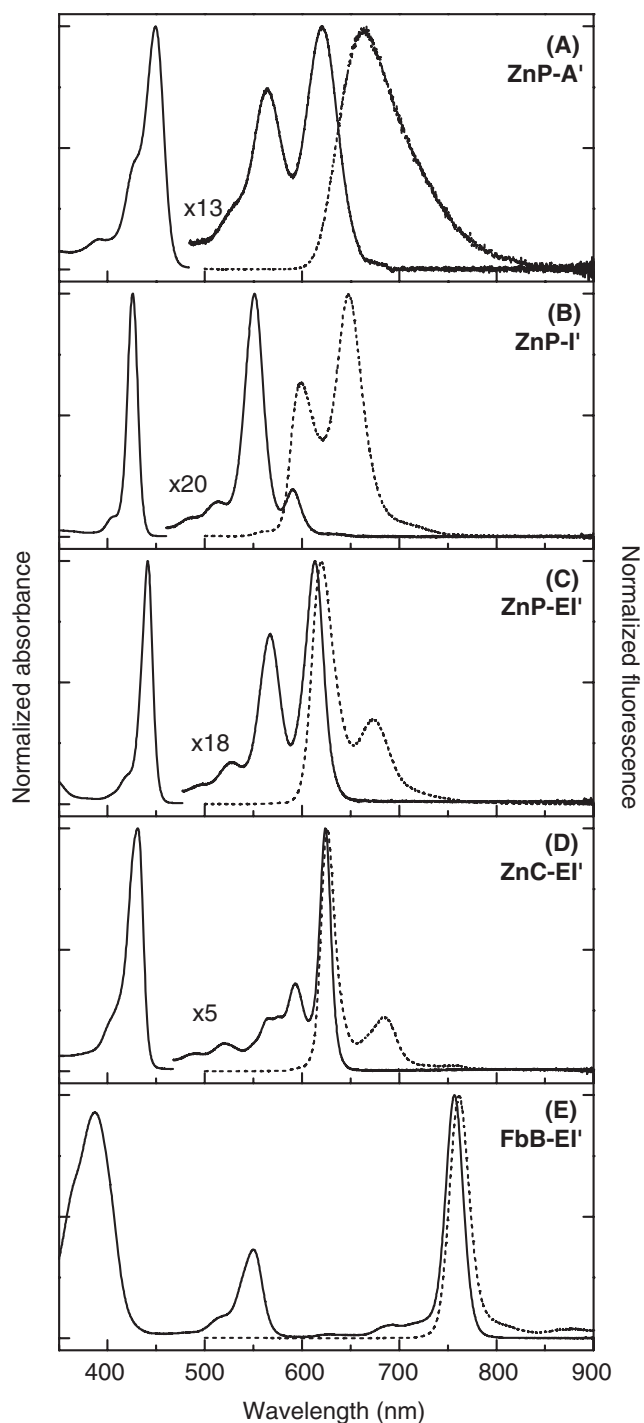


**Figure 2.** Normalized absorption (solid) and fluorescence (dashed) spectra in toluene at room temperature of (A) **ZnP-A'**, (B) **ZnP-I'**, (C) **ZnP-EI'**, (D) **ZnC-EI'** and (E) **FbB-EI'**.

uration of **ZnP-A'** is provisionally assigned as the *trans*-isomer (wherein the carboxy group is *trans* to the porphyrin) as shown in Chart 2.

**Absorption spectra.** The absorption and fluorescence spectra for compounds **ZnP-I'** (zinc porphyrin), **ZnP-EI'** (15-ethynyl-substituted zinc porphyrin), **ZnP-A'** (15-cyanoacrylate-substituted zinc porphyrin), **ZnC-EI'** (15-ethynyl-substi-

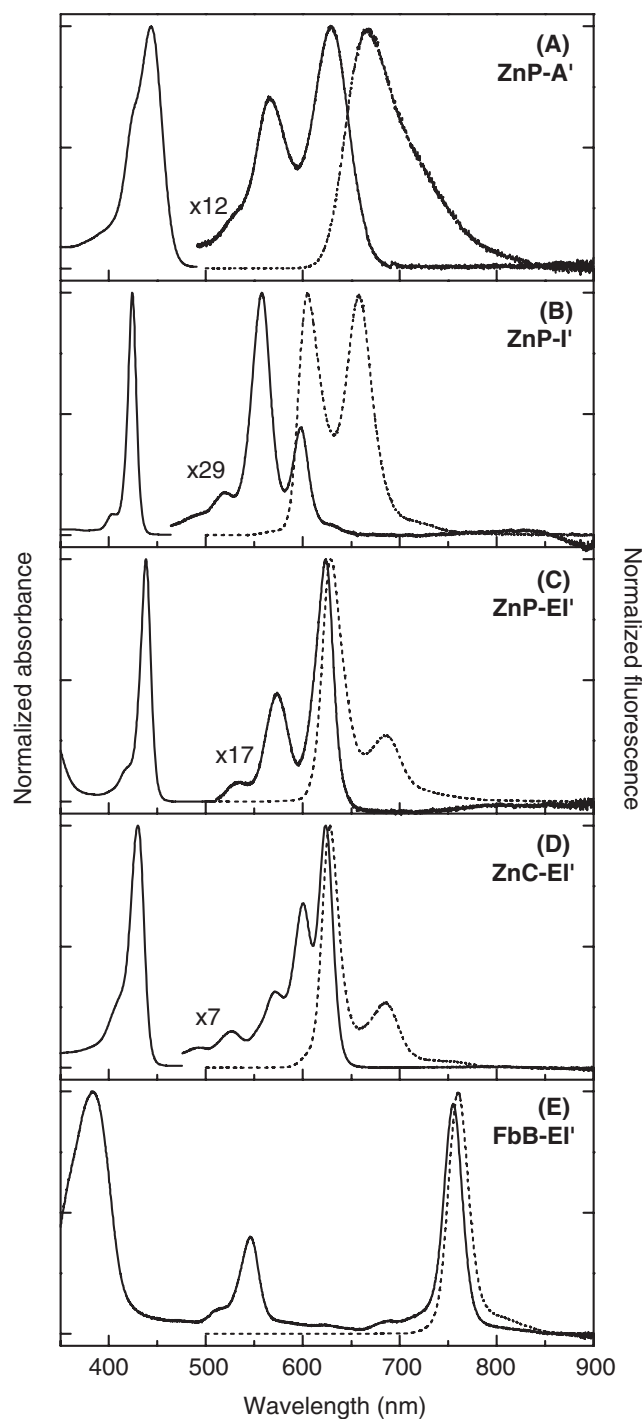


**Figure 3.** Normalized absorption (solid) and fluorescence (dashed) spectra in acetonitrile at room temperature of (A) **ZnP-A'**, (B) **ZnP-I'**, (C) **ZnP-EI'**, (D) **ZnC-EI'** and (E) **FbB-EI'**.

tuted zinc chlorin) and **FbB-EI'** (15-ethynyl-substituted free base bacteriochlorin) in toluene are shown in Fig. 2. Analogous data for the compounds in acetonitrile are given in Fig. 3. The absorption spectra for all the compounds contain a near-UV Soret (*B*) band and a series of *Q* bands to longer wavelengths. For the porphyrins, the long-wavelength absorption band represents the degenerate  $Q_{x,y}(0,0)$  transitions, whereas the band for the chlorin and bacteriochlorin is the

$Q_y(0,0)$  transition (81,82). The band positions and assignments are given in Table 1, which also presents the peak intensity ratio ( $I_B/I_Q$ ) of the *B* and  $Q_y(0,0)$  bands. The table also gives estimates for the molar absorption (extinction) coefficients ( $\epsilon$ ) on the basis of data for related compounds that we have studied previously, including Zn(II)-tetraphenylporphyrin (**ZnTPP**) (70,83) and Zn(II)-5-(4-ethynylphenyl)-10,15,20-triphenylporphyrin (**ZnU**) (84); similarly, the values for the three porphyrins in MeCN were estimated on the basis of data for **ZnU** in benzonitrile (84). These estimates are used below to obtain the radiative rate constant for decay of the  $S_1$  excited state of each compound, which can be compared with values derived from fluorescence yields and excited-state lifetimes. Such comparisons provide cross-checks of the various parameters, including the molar absorption coefficients, for which direct measurement errors of  $\pm 30\%$  or more are common.

The longest-wavelength *Q* absorption band for the compounds in toluene shows a progressive redshift in position ( $\lambda$ ) and increase in peak intensity with respect to the Soret (*B*) band along the series **ZnP-I'** ( $\lambda = 591$  nm;  $I_B/I_Q = 106$ ) < **ZnP-EI'** (614 nm; 18) < **ZnP-A'** (621 nm; 13) < **ZnC-EI'** (624 nm; 4.8) < **FbB-EI'** (757 nm; 0.93) (Fig. 2). The largest combined redshift and intensification of the visible absorption bands are observed upon (i) incorporation of the cyanoacrylate tether in the porphyrin (**ZnP-A'** versus **ZnP-I'**), and (ii) progressing from chlorin to bacteriochlorin (**ZnC-EI'** to **FbB-EI'**). Generally similar trends are observed for the compounds in acetonitrile (Fig. 3).

*Fluorescence spectra, quantum yields and lifetimes.* The  $Q_y(0,0)$  and  $Q_y(0,1)$  fluorescence bands are roughly mirror symmetric to the  $Q_y(0,0)$  and  $Q_y(1,0)$  absorption features. The shifts in the positions of the fluorescence features parallel those in the absorption bands with a change in electronic structure (tether and macrocycle reduction) in both toluene and acetonitrile (Figs. 2 and 3 and Table 1). The exception to this trend is **ZnP-A'**, which shows a much broader spectrum than the other compounds, with a loss of resolution of the vibronic features. In addition, this compound shows an approximately five-fold larger (Stokes) shift between the  $Q(0,0)$  absorption and fluorescence features than the other two porphyrins, and an even larger difference compared to the chlorin and bacteriochlorin (Table 1).

Along the series of compounds in toluene, the fluorescence quantum yield ( $\Phi_f$ ) increases in the following order: **ZnP-I'** (0.033) < **ZnP-A'** (0.063) < **ZnP-EI'** (0.12)  $\sim$  **ZnC-EI'** (0.12) < **FbB-EI'** (0.16). The lifetime of the lowest excited singlet state increases in the order: **ZnP-A'** < (0.98 ns) < **ZnP-I'** (2.3 ns) < **ZnP-EI'** (2.5 ns) < **ZnC-EI'** (2.6 ns) < **FbB-EI'** (5.3 ns). These values for the porphyrins can be compared with that of **ZnTPP** [ $\Phi_f = 0.030$  (70);  $\tau = 2.1$  ns (85)]. Comparable trends in fluorescence quantum yield and excited singlet-state lifetime are observed in acetonitrile (Table 2). Close examination of these data indicates that the fluorescence quantum yield ( $\Phi_f$ ) and lifetime ( $\tau$ ) for **ZnP-A'** do not follow the same trend as the other four compounds. For example, the fluorescence quantum yield for **ZnP-A'** is greater than that for **ZnP-I'** (0.063 versus 0.033), but the reverse is true for the excited-state lifetime (0.98 versus 2.3 ns).

*Excited-state decay properties.* The fluorescence quantum yield and excited-state lifetime often, but not always, parallel one another among a set of tetrapyrrole compounds. A

**Table 1.** Absorption and fluorescence spectral data.\*

| Compound       | Solvent | $B_{\max}$     |   | $Q_x(1,0)$ absn |   | $Q_x(0,0)$ absn |   | $Q_y(0,0)$ absn |   | $(I_B/I_Q)^\dagger$ absn | $Q_y(0,0)^\ddagger$ emsn | $\Delta\nu^\S$      |
|----------------|---------|----------------|---|-----------------|---|-----------------|---|-----------------|---|--------------------------|--------------------------|---------------------|
|                |         | $\lambda$ (nm) | $\epsilon$ (mM <sup>-1</sup> cm <sup>-1</sup> ) | $\lambda$ (nm)  | $\epsilon$ (mM <sup>-1</sup> cm <sup>-1</sup> ) | $\lambda$ (nm)  | $\epsilon$ (mM <sup>-1</sup> cm <sup>-1</sup> ) | $\lambda$ (nm)  | $\epsilon$ (mM <sup>-1</sup> cm <sup>-1</sup> ) |                          | $\lambda$ (nm)           | (cm <sup>-1</sup> ) |
| <b>ZnP-A'</b>  | Toluene | 449            | 414   | 565             | 23  | 621             | 31  | 621             | 31  | 13                       | 663                      | 1020                |
|                | MeCN    | 443            | 322   | 565             | 19  | 630             | 27  | 630             | 27  | 12                       | 667                      | 880                 |
| <b>ZnP-I'</b>  | Toluene | 426            | 475   | 551             | 23  | 591             | 4.5   | 591             | 4.5   | 106                      | 599                      | 230                 |
|                | MeCN    | 424            | 542   | 558             | 19  | 598             | 8.4   | 598             | 8.4   | 65                       | 605                      | 190                 |
| <b>ZnP-EI'</b> | Toluene | 441            | 599   | 567             | 23  | 614             | 33  | 614             | 33  | 18                       | 620                      | 180                 |
|                | MeCN    | 438            | 720   | 573             | 19  | 624             | 43  | 624             | 43  | 17                       | 629                      | 130                 |
| <b>ZnC-EI'</b> | Toluene | 431            | 213   | 520             | 4.8   | 565             | 9.4   | 624             | 44  | 4.8                      | 626                      | 50                  |
|                | MeCN    | 430            | 188   | 526             | 3.9   | 571             | 8.2   | 624             | 26  | 7.2                      | 628                      | 100                 |
| <b>FbB-EI'</b> | Toluene | 387            | 116   | 517             | 11  | 550             | 44  | 757             | 120   | 0.93                     | 761                      | 70                  |
|                | MeCN    | 384            | 113   | 513             | 14  | 546             | 47  | 755             | 108   | 1.1                      | 761                      | 90                  |

\*All measurements were performed at room temperature in toluene or acetonitrile (MeCN). The molar absorption coefficient for each compound was derived from the relative amplitudes of the bands (Figs. 2 and 3), using the value at a specific band maximum that was estimated as follows. The value at the  $Q_{x,y}(1,0)$  maximum of **ZnP-A'**, **ZnP-I'** and **ZnP-EI'** in toluene is based on data for benchmark porphyrins **ZnTPP** (70,83) and **ZnU** (84); similarly, the value for the three porphyrins in MeCN was estimated based on data for **ZnU** in benzonitrile (84). The value for **ZnC-EI'** in toluene at the  $Q_y(0,0)$  band is based on the data for Zn(II)-17,18-dihydro-10-mesityl-18,18-dimethyl-5-(4-methylphenyl)porphyrin (**ZnC-T<sup>5</sup>M<sup>10</sup>**) in toluene (23). The value estimated for **FbB-EI'** in toluene is based on the data for 5-methoxy-8,8,18,18-tetramethyl-2,12-bis(4-methylphenyl)bacteriochlorin (**MeO-BC**) in toluene (35). The values for **ZnC-EI'** and **FbB-EI'** at the  $Q_y(0,0)$  maximum in MeCN are based on those obtained for these compounds in benzonitrile determined here (see Materials and Methods).  $\dagger$ Ratio of the peak intensities of the Soret (*B*) and  $Q_x(0,0)$  absorption bands.  $\ddagger$  $Q_y(0,0)$  fluorescence maximum.  $\S$ Difference in the energies of the  $Q_y(0,0)$  absorption and fluorescence bands (*i.e.* the Stokes shift).

**Table 2.** Summary of photophysical data.

| Cmpd           | Solvent | $\Phi_f^*$ | $\tau_f^\dagger$ (ns) | $[(k_f)^{-1}]^\ddagger$ (ns) | $[(k_f^{SB})^{-1}]^\S$ (ns) | $[(k_{nr})^{-1}]^\parallel$ (ns) | $[(k_{nr}^{SB})^{-1}]^\P$ (ns) |
|----------------|---------|------------|-----------------------|------------------------------|-----------------------------|----------------------------------|--------------------------------|
| <b>ZnTPP</b>   | Toluene | 0.030#     | 2.1**                 | 70                           | 57                          | 2.2                              | 2.2                            |
| <b>ZnP-A'</b>  | Toluene | 0.063      | 0.98                  | 16                           | 24                          | 1.0                              | 1.0                            |
|                | MeCN    | 0.044      | 0.96                  | 22                           | 33                          | 1.0                              | 1.0                            |
| <b>ZnP-I'</b>  | Toluene | 0.033      | 2.3                   | 70                           | 56                          | 2.4                              | 2.4                            |
|                | MeCN    | 0.026      | 2.1                   | 79                           | 68                          | 2.2                              | 2.2                            |
| <b>ZnP-EI'</b> | Toluene | 0.12       | 2.5                   | 21                           | 28                          | 2.8                              | 2.7                            |
|                | MeCN    | 0.098      | 2.4                   | 24                           | 37                          | 2.7                              | 2.6                            |
| <b>ZnC-EI'</b> | Toluene | 0.12       | 2.6                   | 21                           | 24                          | 3.0                              | 2.9                            |
|                | MeCN    | 0.11       | 2.9                   | 25                           | 35                          | 3.3                              | 3.2                            |
| <b>FbB-EI'</b> | Toluene | 0.16       | 5.3                   | 32                           | 16                          | 6.4                              | 7.9                            |
|                | MeCN    | 0.14       | 5.6                   | 41                           | 19                          | 6.5                              | 7.9                            |

\*Fluorescence quantum yield ( $\pm 15\%$ ) determined using *B*-band excitation and chlorophyll *a* in benzene ( $\Phi_f = 0.325$ ) (71) as a standard for **FbB-EI'** and **ZnC-EI'**, and **ZnTPP** in toluene ( $\Phi_f = 0.030$ ) (70) as a standard for **ZnP-EI'**, **ZnP-I'** and **ZnP-A'**.  $\dagger$ Excited singlet-state lifetime ( $\pm 10\%$ ) determined using fluorescence modulation spectroscopy and *B*-band excitation.  $\ddagger$ The time constant (inverse of rate constant) for the radiative (spontaneous fluorescence) decay pathway of the excited singlet obtained using the fluorescence quantum yield and lifetime *via* the equation  $(k_f)^{-1} = \tau/\Phi_f$ .  $\S$ The time constant (inverse of rate constant) for the radiative decay pathway of the excited singlet obtained using the Strickler–Berg relationship (Eq. 6) and the absorption and fluorescence spectra (Figs. 2 and 3 and Table 1).  $\parallel$ The overall time constant (inverse of the combined rate constant) for the nonradiative decay pathways (internal conversion plus intersystem crossing) of the excited singlet obtained using Eq. 5.  $\P$ The overall time constant (inverse of the combined rate constant) for the nonradiative decay pathways (internal conversion plus intersystem crossing) of the excited singlet obtained using Eq. 8. #From Seybold and Gouterman (70). \*\*From Tomizaki *et al.* (85).

parallelism is generally expected because these two observables are related by the rate constants for the radiative (spontaneous fluorescence) ( $k_f$ ) and internal conversion ( $k_{ic}$ ) decay pathways of the excited singlet state to the ground state, and for intersystem crossing ( $k_{isc}$ ) to the triplet excited state by the following equations.

$$\tau = \frac{1}{k_f + k_{ic} + k_{isc}} \quad (1)$$

$$\Phi_f = \frac{k_f}{k_f + k_{ic} + k_{isc}} \quad (2)$$

Combining Eqs. (1) and (2) gives the radiative rate constant *via* the expression

$$k_f = \frac{\Phi_f}{\tau} \quad (3)$$

An estimate for  $k_f$  can be obtained for each compound in a given solvent using the measured values for  $\Phi_f$  and  $\tau$ . The inverse of  $k_f$  (units of nanoseconds) is listed in the fifth column of Table 2. It is also convenient to combine the rate constants for the two nonradiative decay routes of the lowest excited singlet state to obtain

$$k_{nr} = k_{ic} + k_{isc}. \quad (4)$$

Combining Eqs. (4) and (1) gives

$$k_{nr} = \tau^{-1} - k_f. \quad (5)$$

An estimate for  $k_{nr}$  can be obtained for each compound in a given solvent using the measured value of  $\tau$  and the value of  $k_f$  obtained using Eq. (3) (seventh column of Table 2).

Another estimate for the radiative rate constant can be obtained by integrating the absorption profile for the  $S_0 \rightarrow S_1$  vibronic transitions. For this purpose, it is common to utilize the Strickler–Berg relationship (86), which takes into account the fact that the  $S_0 \leftrightarrow S_1$  (induced) absorption and (spontaneous fluorescence) emission bands are not superimposed but obey an (approximate) mirror symmetry relationship. The Strickler–Berg formula is as follows:

$$k_f^{SB} = 2.88 \times 10^{-9} n^2 \langle \bar{\nu}_f^{-3} \rangle_{Av}^{-1} \frac{g_l}{g_u} \int \frac{\epsilon}{\bar{\nu}} d\bar{\nu} \quad (6)$$

Here,  $n$  is the refractive index of the solvent and  $g_l/g_u$  is the ratio of the degeneracy of the lower ( $S_0$ ) state to that of the upper ( $S_1$ ) state. The integration is over the  $S_0 \rightarrow S_1$  absorption profile (*i.e.* encompassing the  $Q_x(0,0)$  and  $Q_y(1,0)$  bands) expressed as the molar absorption coefficient ( $\epsilon$ ) versus the wavenumber ( $\bar{\nu}$ ) position. The quantity in Eq. 6 in brackets is derived from the fluorescence profile as follows:

$$\langle \bar{\nu}_f^{-3} \rangle_{Av}^{-1} = \frac{\int I(\bar{\nu}) d\bar{\nu}}{\int \bar{\nu}^{-3} I(\bar{\nu}) d\bar{\nu}} \quad (7)$$

The calculation of  $k_f^{SB}$  for each of the five tetrapyrrole esters utilized the absorption and fluorescence spectra in Figs. 2 and 3 along with the estimated molar absorption coefficients in Table 1. The calculations were performed both using Origin (Microcal) software and PhotochemCad (2). Due to the overlap of the  $x$ - and  $y$ -polarized  $Q$ -band absorption transitions of porphyrins **ZnP-A'**, **ZnP-EI'** and **ZnP-I'**, a degeneracy ratio of 1/2 was used for each of these compounds (and the reference compound **ZnTPP**). The degeneracy ratio is 1 for **ZnC-EI'** and for **FbB-EI'**. The values for the inverse of the  $k_f^{SB}$  (units of nanoseconds) calculated using the Strickler–Berg analysis are listed in the sixth column of Table 2. In analogy with the logic underpinning Eq. (4), the value of  $k_f^{SB}$  can be used to obtain a second measure of the effective nonradiative excited-state decay rate as follows:

$$k_{nr}^{SB} = \tau^{-1} - k_f^{SB}. \quad (8)$$

The results are listed in the last column of Table 2.

Inspection of Table 2 indicates that there is generally good agreement of the values for the radiative rate obtained from the measured fluorescence lifetime and yield ( $k_f$ ) and that obtained from the Strickler–Berg analysis of the absorption and fluorescence profiles ( $k_f^{SB}$ ). The largest deviation is found for the free base bacteriochlorin **FbB-EI'**. The agreement between the values is good considering the errors in the various measurements and in the assumptions underlying the Strickler–Berg analysis. The latter can be an issue for some porphyrins because the overtone vibronic transitions derive most of their intensity from Herzberg–Teller coupling rather than from Franck–Condon overlap, which may not be the

same in the  $S_0$  and  $S_1$  states (breaking the mirror symmetry relationship).

Comparisons among the values obtained for the compounds in toluene are useful in showing reasonable consistency of the various measurements and parameters. For the porphyrin bearing the aryl ester tether (**ZnP-I'**), the radiative rates  $k_f = (70 \text{ ns})^{-1}$  and  $k_f^{SB} = (56 \text{ ns})^{-1}$  agree well with each other. These values are also in concert with those for zinc tetraphenylporphyrin (**ZnTPP**), namely  $k_f^{SB} \sim (60 \text{ ns})^{-1}$  obtained by Seybold and Gouterman (70) and  $k_f^{SB} = (57 \text{ ns})^{-1}$  and  $k_f = (70 \text{ ns})^{-1}$  obtained here (Table 2). For the porphyrin bearing the ethynylaryl ester tether (**ZnP-EI'**), the radiative rates  $k_f = (21 \text{ ns})^{-1}$  and  $k_f^{SB} = (28 \text{ ns})^{-1}$  agree well, as do those for the porphyrin bearing the cyanoacrylate tether (**ZnP-A'**), for which  $k_f = (16 \text{ ns})^{-1}$  and  $k_f^{SB} = (24 \text{ ns})^{-1}$ . Thus, amongst the three zinc porphyrins, both  $k_f$  and  $k_f^{SB}$  increase in the order **ZnP-I'** < **ZnP-EI'** < **ZnP-A'**. This trend reflects an increasing radiative probability, which is in keeping with the increased intensity of the  $Q_{x,y}(0,0)$  band that occurs (in parallel with a redshift) along this series (Figs. 2 and 3 and Table 1).

The rates  $k_f = (21 \text{ ns})^{-1}$  and  $k_f^{SB} = (24 \text{ ns})^{-1}$  for zinc chlorin **ZnC-EI'** are both comparable to those for the porphyrin analog **ZnP-EI'**. The deviation between the two estimates for the radiative rate is largest for the free base bacteriochlorin **FbB-EI'** and the reason is unclear. In particular, the value of  $k_f = (32 \text{ ns})^{-1}$  is comparable to the average value  $k_f = (27 \text{ ns})^{-1}$  obtained from the fluorescence yield and excited-state lifetime for a series of synthetic free base and zinc bacteriochlorins (H. L. Kee and D. Holten, unpublished). On the other hand, the shorter value,  $k_f^{SB} = (16 \text{ ns})^{-1}$ , obtained for **FbB-EI'** from the Strickler–Berg analysis is consistent with the greater oscillator strength in the  $Q_y$  absorption manifold compared to that for zinc chlorin **ZnC-EI'** (Table 1).

The  $S_1 \rightarrow S_0$  radiative decay route is in competition with the  $S_1 \rightarrow S_0$  internal conversion and  $S_1 \rightarrow T_1$  intersystem-crossing nonradiative decay pathways. The net rate for the latter two routes [Eq. (5)] is virtually the same for porphyrin **ZnP-I'** [ $k_{nr} = (2.2 \text{ ns})^{-1}$ ] and the reference compound **ZnTPP** (Table 1). The effective nonradiative decay for arylethynyl porphyrin **ZnP-EI'** [ $k_{nr} = (2.8 \text{ ns})^{-1}$ ] and arylethynyl chlorin **ZnC-EI'** [ $k_{nr} = (3.0 \text{ ns})^{-1}$ ] is only modestly slower, while that for free base bacteriochlorin **FbB-EI'** [ $k_{nr} = (6.4 \text{ ns})^{-1}$ ] is considerably reduced. The largest effective nonradiative decay rate is found for porphyrin **ZnP-A'** [ $k_{nr} \sim (1 \text{ ns})^{-1}$ ]. This difference is most likely due to enhanced internal conversion to the ground state. This possibility is consistent with the much larger (Stokes) shift between the  $Q(0,0)$  absorption and fluorescence bands (Table 1) and the much broader bands in both spectra for this compound compared to the other tetrapyrroles studied here. These combined data are analogous to those observed for porphyrins that are rendered nonplanar by steric interactions involving the substituents, leading to increased macrocycle conformational excursions, which may be enhanced upon photoexcitation (87–89). Regardless of the ultimate origin, the presence of the cyanoacrylate group in the tether for **ZnP-A'** (and presumably the cyanoacrylic acid group in **ZnP-A**) results in enhanced nonradiative decay that shortens the excited-state lifetime. However, this lifetime is still sufficiently long ( $\sim 1 \text{ ns}$ ) that effective electron transfer from the photoexcited sensitizer to a semiconductor surface should be possible, as is the case for the other tetrapyrrole

sensitizers studied here, which have even longer excited-state lifetimes. The effect of electronic coupling through the linker and thermodynamic considerations owing to the different macrocycles is the subject of a companion article in which the contributions of the light-harvesting and redox characteristics to solar-cell efficiency among the five sensitizers are analyzed (3).

*Acknowledgements*—This research was supported by grants from the Division of Chemical Sciences, Office of Basic Energy Sciences, Office of Energy Research, U.S. Department of Energy to D.F.B. (DE-FG02-05ER15660), D.H. (DE-FG02-05ER15661) and J.S.L. (DE-FG02-96ER14632). Mass spectra were obtained at the Mass Spectrometry Laboratory for Biotechnology at North Carolina State University. Partial funding for the NCSU Facility was obtained from the North Carolina Biotechnology Center and the NSF.

## REFERENCES

- Gouterman, M. (1978) Optical spectra and electronic structure of porphyrins and related rings. In *The Porphyrins*, Vol. 3 (Edited by D. Dolphin), pp. 1–165. Academic Press, New York.
- Dixon, J. M., M. Taniguchi and J. S. Lindsey (2005) PhotochemCAD 2. A refined program with accompanying spectral databases for photochemical calculations. *Photochem. Photobiol.* **81**, 212–213.
- Stromberg, J. R., A. Marton, H. L. Kee, C. Kirmaier, J. R. Diers, C. Muthiah, M. Taniguchi, J. S. Lindsey, D. F. Bocian, G. J. Meyer and D. Holten (2007) Examination of tethered porphyrin, chlorin, and bacteriochlorin molecules in mesoporous metal-oxide solar cells. *J. Phys. Chem. C* **111**, doi:10.1021/jp0749928.
- Vicente, M. G. H. (2001) Reactivity and functionalization of  $\beta$ -substituted porphyrins and chlorins. In *The Porphyrin Handbook*, Vol. 1 (Edited by K. M. Kadish, K. M. Smith and R. Guilard), pp. 149–199. Academic Press, San Diego, CA.
- Jaquinod, L. (2001) Functionalization of 5,10,15,20-tetra-substituted porphyrins. In *The Porphyrin Handbook*, Vol. 1 (Edited by K. M. Kadish, K. M. Smith and R. Guilard), pp. 201–237. Academic Press, San Diego, CA.
- Hynninen, P. H. (1991) Chemistry of chlorophylls: Modifications. In *Chlorophylls* (Edited by H. Scheer), pp. 145–209. CRC Press, Boca Raton, FL.
- Osuka, A., Y. Wada and S. Shinoda (1996) Covalently linked pyropheophorbide dimers as models of the special pair in the photosynthetic reaction center. *Tetrahedron* **52**, 4311–4326.
- Tamiaki, H. and M. Kouraba (1997) Synthesis of chlorophyll-*a* homologs by Wittig and Knoevenagel reactions with methyl pyropheophorbide-*d*. *Tetrahedron* **53**, 10677–10688.
- Gerlach, B., S. E. Brantley and K. M. Smith (1998) Novel synthetic routes to 8-vinyl chlorophyll derivatives. *J. Org. Chem.* **63**, 2314–2320.
- Kozyrev, A. N., J. L. Alderfer and B. C. Robinson (2003) Pyrazolinyl and cyclopropyl derivatives of protoporphyrin IX and chlorins related to chlorophyll *a*. *Tetrahedron* **59**, 499–504.
- Li, G., A. Graham, Y. Chen, M. P. Dobhal, J. Morgan, G. Zheng, A. Kozyrev, A. Oseroff, T. J. Dougherty and R. K. Pandey (2003) Synthesis, comparative photosensitizing efficacy, human serum albumin (site II) binding ability, and intracellular localization characteristics of novel benzobacteriochlorins derived from *vic*-dihydroxybacteriochlorins. *J. Med. Chem.* **46**, 5349–5359.
- Feofanov, A. V., A. I. Nazarova, T. A. Karmakova, A. D. Plyutinskaya, A. I. Grishin, R. I. Yakubovskaya, V. S. Lebedeva, R. D. Ruziev, A. F. Mironov, J.-C. Maurizot and P. Vigny (2004) Photobiological properties of 13,15-*N*-(carboxymethyl)- and 13,15-*N*-(2-carboxyethyl)cycloimide derivatives of chlorin *p6*. *Russ. J. Bioorg. Chem.* **30**, 374–384.
- Balaban, T. S., H. Tamiaki and A. R. Holzwarth (2005) Chlorins programmed for self-assembly. *Top. Curr. Chem.* **258**, 1–38.
- Wang, J.-J., K. Imafuku, Y. K. Shim and G.-J. Jiang (2005) Synthesis of 3<sup>2</sup>-phenyl-substituted methyl *E/Z*-pyropheophorbide-*a*'s from methyl *E/Z*-pyropheophorbide-*a* 13<sup>1</sup>-ketoximes. *J. Heterocycl. Chem.* **42**, 835–840.
- Kelley, R. F., M. J. Tauber and M. R. Wasielewski (2006) Intramolecular electron transfer through the 20-position of a chlorophyll *a* derivative: An unexpectedly efficient conduit for charge transport. *J. Am. Chem. Soc.* **128**, 4779–4791.
- Wasielewski, M. R. and W. A. Svec (1980) Synthesis of covalently linked dimeric derivatives of chlorophyll *a*, pyrochlorophyll *a*, chlorophyll *b*, and bacteriochlorophyll *a*. *J. Org. Chem.* **45**, 1969–1974.
- Struck, A., E. Cmiel, I. Katheder, W. Schäfer and H. Scheer (1992) Bacteriochlorophylls modified at position C-3: Long-range intramolecular interaction with position C-13<sup>2</sup>. *Biochim. Biophys. Acta* **1101**, 321–328.
- Mironov, A. F., M. A. Grin, A. G. Tsiprovskii, A. V. Segenevich, D. V. Dzardanov, K. V. Golovin, A. A. Tsygankov and Ya K. Shim (2003) New photosensitizers of bacteriochlorin series for photodynamic cancer therapy. *Russ. J. Bioorg. Chem.* **29**, 190–197.
- Mironov, A. F., M. A. Grin, A. G. Tsiprovskiy, V. V. Kachala, T. A. Karmakova, A. D. Plyutinskaya and R. I. Yakubovskaya (2003) New bacteriochlorin derivatives with a fused *N*-aminoimide ring. *J. Porphyrins Phthalocyanines* **7**, 725–730.
- Kozyrev, A. N., Y. Chen, L. N. Goswami, W. A. Tabaczynski and R. K. Pandey (2006) Characterization of porphyrins, chlorins, and bacteriochlorins formed via allomerization of bacteriochlorophyll *a*. Synthesis of highly stable bacteriopurpurinimides and their metal complexes. *J. Org. Chem.* **71**, 1949–1960.
- Sasaki, S.-I. and H. Tamiaki (2006) Synthesis and optical properties of bacteriochlorophyll-*a* derivatives having various C3 substituents on the bacteriochlorin  $\pi$ -system. *J. Org. Chem.* **71**, 2648–2654.
- Gryshuk, A., Y. Chen, L. N. Goswami, S. Pandey, J. R. Missert, T. Ohulchanskyy, W. Potter, P. N. Prasad, A. Oseroff and R. K. Pandey (2007) Structure-activity relationship among purpurinimides and bacteriopurpurinimides: Trifluoromethyl substituent enhanced the photosensitizing efficacy. *J. Med. Chem.* **50**, 1754–1767.
- Strachan, J.-P., D. F. O'Shea, T. Balasubramanian and J. S. Lindsey (2000) Rational synthesis of meso-substituted chlorin building blocks. *J. Org. Chem.* **65**, 3160–3172.
- Balasubramanian, T., J.-P. Strachan, P. D. Boyle and J. S. Lindsey (2000) Rational synthesis of  $\beta$ -substituted chlorin building blocks. *J. Org. Chem.* **65**, 7919–7929.
- Taniguchi, M., D. Ra, G. Mo, T. Balasubramanian and J. S. Lindsey (2001) Synthesis of meso-substituted chlorins via tetrahydrobilene-*a* intermediates. *J. Org. Chem.* **66**, 7342–7354.
- Taniguchi, M., H.-J. Kim, D. Ra, J. K. Schwartz, C. Kirmaier, E. Hindin, J. R. Diers, S. Prathapan, D. F. Bocian, D. Holten and J. S. Lindsey (2002) Synthesis and electronic properties of regioisomerically pure oxochlorins. *J. Org. Chem.* **67**, 7329–7342.
- Taniguchi, M., M. N. Kim, D. Ra and J. S. Lindsey (2005) Introduction of a third meso substituent into diaryl chlorins and oxochlorins. *J. Org. Chem.* **70**, 275–285.
- Laha, J. K., C. Muthiah, M. Taniguchi, B. E. McDowell, M. Ptaszek and J. S. Lindsey (2006) Synthetic chlorins bearing auxochromes at the 3- and/or 13-positions. *J. Org. Chem.* **71**, 4092–4102.
- Laha, J. K., C. Muthiah, M. Taniguchi and J. S. Lindsey (2006) A new route for installing the isocyclic ring in chlorins yielding 13<sup>1</sup>-oxophorbines. *J. Org. Chem.* **71**, 7049–7052.
- Ptaszek, M., B. E. McDowell, M. Taniguchi, H.-J. Kim and J. S. Lindsey (2007) Sparsely substituted chlorins as core constructs in chlorophyll analogue chemistry. Part 1: Synthesis. *Tetrahedron* **63**, 3826–3839.
- Taniguchi, M., M. Ptaszek, B. E. McDowell and J. S. Lindsey (2007) Sparsely substituted chlorins as core constructs in chlorophyll analogue chemistry. Part 2: Derivatization. *Tetrahedron* **63**, 3840–3849.
- Taniguchi, M., M. Ptaszek, B. E. McDowell, P. D. Boyle and J. S. Lindsey (2007) Sparsely substituted chlorins as core constructs in chlorophyll analogue chemistry. Part 3: Spectral and structural properties. *Tetrahedron* **63**, 3850–3863.
- Kee, H. L., C. Kirmaier, Q. Tang, J. R. Diers, C. Muthiah, M. Taniguchi, J. K. Laha, M. Ptaszek, J. S. Lindsey, D. F. Bocian

- and D. Holten (2007) Effects of substituents on synthetic analogs of chlorophylls. Part 1: Synthesis, vibrational properties and excited-state decay characteristics. *Photochem. Photobiol.* **83**, 1110–1124.
34. Kee, H. L., C. Kirmaier, Q. Tang, J. R. Diers, C. Muthiah, M. Taniguchi, J. K. Laha, M. Ptaszek, J. S. Lindsey, D. F. Bocian and D. Holten (2007) Effects of substituents on synthetic analogs of chlorophylls. Part 2: Redox properties, optical spectra and electronic structure. *Photochem. Photobiol.* **83**, 1125–1143.
  35. Kim, H.-J. and J. S. Lindsey (2005) De novo synthesis of stable tetrahydroporphyrinic macrocycles: Bacteriochlorins and a tetradehydrochlorin. *J. Org. Chem.* **70**, 5475–5486.
  36. Fan, D., M. Taniguchi and J. S. Lindsey (2007) Regioselective 15-bromination and functionalization of a stable synthetic bacteriochlorin. *J. Org. Chem.* **72**, 5350–5357.
  37. Kay, A. and M. Grätzel (1993) Artificial photosynthesis. I. Photosensitization of TiO<sub>2</sub> solar cells with chlorophyll derivatives and related natural porphyrins. *J. Phys. Chem.* **97**, 6272–6277.
  38. Boschloo, G. K. and A. Goossens (1996) Electron trapping in porphyrin-sensitized porous nanocrystalline TiO<sub>2</sub> electrodes. *J. Phys. Chem.* **100**, 19489–19494.
  39. Gervaldo, M., F. Fungo, E. N. Durantini, J. J. Silber, L. Sereno and L. Otero (2005) Carboxyphenyl metalloporphyrins as photosensitizers of semiconductor film electrodes. A study of the effect of different central metals. *J. Phys. Chem. B* **109**, 20953–20962.
  40. Rochford, J., D. Chu, A. Hagfeldt and E. Galoppini (2007) Tetrachelate porphyrin chromophores for metal oxide semiconductor sensitization: Effect of the spacer length and anchoring group position. *J. Am. Chem. Soc.* **129**, 4655–4665.
  41. Nazeeruddin, M. K., R. Humphry-Baker, D. L. Officer, W. M. Campbell, A. K. Burrell and M. Grätzel (2004) Application of metalloporphyrins in nanocrystalline dye-sensitized solar cells for conversion of sunlight into electricity. *Langmuir* **20**, 6514–6517.
  42. Campbell, W. M., A. K. Burrell, D. L. Officer and K. W. Jolley (2004) Porphyrins as light harvesters in the dye-sensitized TiO<sub>2</sub> solar cell. *Coord. Chem. Rev.* **248**, 1363–1379.
  43. Muthukumar, K., R. S. Loewe, A. Ambroise, S.-I. Tamaru, Q. Li, G. Mathur, D. F. Bocian, V. Misra and J. S. Lindsey (2004) Porphyrins bearing arylphosphonic acid tethers for attachment to oxide surfaces. *J. Org. Chem.* **69**, 1444–1452.
  44. Loewe, R. S., A. Ambroise, K. Muthukumar, K. Padmaja, A. B. Lysenko, G. Mathur, Q. Li, D. F. Bocian, V. Misra and J. S. Lindsey (2004) Porphyrins bearing mono or tripodal benzylphosphonic acid tethers for attachment to oxide surfaces. *J. Org. Chem.* **69**, 1453–1460.
  45. Wang, Q., W. M. Campbell, E. E. Bonfantani, K. W. Jolley, D. L. Officer, P. J. Walsh, K. Gordon, R. Humphry-Baker, M. K. Nazeeruddin and M. Grätzel (2005) Efficient light harvesting by using green Zn-porphyrin-sensitized nanocrystalline TiO<sub>2</sub> films. *J. Phys. Chem. B* **109**, 15397–15409.
  46. Schmidt-Mende, L., W. M. Campbell, Q. Wang, K. W. Jolley, D. L. Officer, M. K. Nazeeruddin and M. Grätzel (2005) Zn-porphyrin-sensitized nanocrystalline TiO<sub>2</sub> heterojunction photovoltaic cells. *Chemphyschem* **6**, 1253–1258.
  47. Giribabu, L., Ch. V. Kumar and P. Y. Reddy (2006) Porphyrin-rhodanine dyads for dye sensitized solar cells. *J. Porphyrins Phthalocyanines* **10**, 1007–1016.
  48. Morisue, M., N. Haruta, D. Kalita and Y. Kobuke (2006) Efficient charge injection from the S<sub>2</sub> photoexcited state of special-pair mimic porphyrin assemblies anchored on a titanium-modified ITO anode. *Chem. Eur. J.* **12**, 8123–8135.
  49. Lo, C.-F., L. Luo, E. W.-G. Diau, I.-J. Chang and C.-Y. Lin (2006) Evidence for the assembly of carboxyphenylethynyl zinc porphyrins on nanocrystalline TiO<sub>2</sub> surfaces. *Chem. Commun.* 1430–1432.
  50. Eu, S., S. Hayashi, T. Umeyama, A. Oguro, M. Kawasaki, N. Kadota, Y. Matano and H. Imahori (2007) Effects of 5-membered heteroaromatic spacers on structures of porphyrin films and photovoltaic properties of porphyrin-sensitized TiO<sub>2</sub> cells. *J. Phys. Chem. C* **111**, 3528–3537.
  51. Hara, K., M. Kurashige, S. Ito, A. Shinpo, S. Suga, K. Sayama and H. Arakawa (2003) Novel polyene dyes for highly efficient dye-sensitized solar cells. *Chem. Commun.* 252–253.
  52. Hara, K., M. Kurashige, Y. Dan-oh, C. Kasada, A. Shinpo, S. Suga, K. Sayama and H. Arakawa (2003) Design of new coumarin dyes having thiophene moieties for highly efficient organic-dye-sensitized solar cells. *New J. Chem.* **27**, 783–785.
  53. Hoertz, P. G., R. A. Carlisle, G. J. Meyer, D. Wang, P. Piotrowiak and E. Galoppini (2003) Organic rigid-rod linkers for coupling chromophores to metal oxide nanoparticles. *Nano Lett.* **3**, 325–330.
  54. Wang, D., R. Mendelsohn, E. Galoppini, P. G. Hoertz, R. A. Carlisle and G. J. Meyer (2004) Excited state electron transfer from Ru(II) polypyridyl complexes anchored to nanocrystalline TiO<sub>2</sub> through rigid-rod linkers. *J. Phys. Chem. B* **108**, 16642–16653.
  55. Galoppini, E. (2004) Linkers for anchoring sensitizers to semiconductor nanoparticles. *Coord. Chem. Rev.* **248**, 1283–1297.
  56. Lamberto, M., C. Pagba, P. Piotrowiak and E. Galoppini (2005) Synthesis of novel rigid-rod and tripodal azulene chromophores. *Tetrahedron Lett.* **46**, 4895–4899.
  57. Taratula, O., J. Rochford, P. Piotrowiak, E. Galoppini, R. A. Carlisle and G. J. Meyer (2006) Pyrene-terminated phenylene-ethynylene rigid linkers anchored to metal oxide nanoparticles. *J. Phys. Chem. B* **110**, 15734–15741.
  58. Srinivasan, N., C. A. Haney, J. S. Lindsey, W. Zhang and B. T. Chait (1999) Investigation of MALDI-TOF mass spectrometry of diverse synthetic metalloporphyrins, phthalocyanines, and metalloporphyrin arrays. *J. Porphyrins Phthalocyanines* **3**, 283–291.
  59. Zaidi, S. H. H., R. Fico Jr and J. S. Lindsey (2006) Investigation of streamlined syntheses of porphyrins bearing distinct meso substituents. *Org. Process Res. Dev.* **10**, 118–134.
  60. Tamaru, S.-I., L. Yu, W. J. Youngblood, K. Muthukumar, M. Taniguchi and J. S. Lindsey (2004) A tin-complexation strategy for use with diverse acylation methods in the preparation of 1,9-diacetyldipyromethanes. *J. Org. Chem.* **69**, 765–777.
  61. Tomizaki, K.-Y., A. B. Lysenko, M. Taniguchi and J. S. Lindsey (2004) Synthesis of phenylethyne-linked porphyrin dyads. *Tetrahedron* **60**, 2011–2023.
  62. Liu, Z., A. A. Yasseri, R. S. Loewe, A. B. Lysenko, V. L. Malinovsky, Q. Zhao, S. Surthi, Q. Li, V. Misra, J. S. Lindsey and D. F. Bocian (2004) Synthesis of porphyrins bearing hydrocarbon tethers and facile covalent attachment to Si(100). *J. Org. Chem.* **69**, 5568–5577.
  63. Rao, P. D., S. Dhanalekshmi, B. J. Littler and J. S. Lindsey (2000) Rational syntheses of porphyrins bearing up to four different meso substituents. *J. Org. Chem.* **65**, 7323–7344.
  64. Geier, G. R., III, J. B. Callinan, P. D. Rao and J. S. Lindsey (2001) A survey of acid catalysts in dipyrromethanecarbinol condensations leading to meso-substituted porphyrins. *J. Porphyrins Phthalocyanines* **5**, 810–823.
  65. Yu, L. and J. S. Lindsey (2001) Investigation of two rational routes for preparing *p*-phenylene-linked porphyrin trimers. *Tetrahedron* **57**, 9285–9298.
  66. Wagner, R. W., T. E. Johnson, F. Li and J. S. Lindsey (1995) Synthesis of ethyne-linked or butadiyne-linked porphyrin arrays using mild, copper-free, Pd-mediated coupling reactions. *J. Org. Chem.* **60**, 5266–5273.
  67. Wagner, R. W., Y. Ciringh, C. Clausen and J. S. Lindsey (1999) Investigation and refinement of palladium-coupling conditions for the synthesis of diarylethyne-linked multiporphyrin arrays. *Chem. Mater.* **11**, 2974–2983.
  68. Okanuma, M., Y. Ishida, Y. Hase, N. Higashida and T. Enoki (2005) *Aromatic carboxylic acids, acid halides thereof and processes for preparing both*. US Patent 6,949,674 B2.
  69. Lindsey, J. S., S. Prathapan, T. E. Johnson and R. W. Wagner (1994) Porphyrin building blocks for modular construction of bioorganic model systems. *Tetrahedron* **50**, 8941–8968.
  70. Seybold, P. G. and M. Gouterman (1969) Porphyrins XIII: Fluorescence spectra and quantum yields. *J. Mol. Spectrosc.* **31**, 1–13.
  71. Weber, G. and F. W. J. Teale (1957) Determination of the absolute quantum yield of fluorescent solutions. *Trans. Faraday Soc.* **53**, 646–655.
  72. Kee, H. L., C. Kirmaier, L. Yu, P. Thamyongkit, W. J. Youngblood, M. E. Calder, L. Ramos, B. C. Noll, D. F. Bocian, W. R. Scheidt, R. R. Birge, J. S. Lindsey and D. Holten (2005) Structural

- control of the photodynamics of boron-dipyrin complexes. *J. Phys. Chem. B* **109**, 20433–20443.
73. Balakumar, A., K. Muthukumaran and J. S. Lindsey (2004) A new route to *meso*-formyl porphyrins. *J. Org. Chem.* **69**, 5112–5115.
74. Murata, M., S. Watanabe and Y. Masuda (1997) Novel palladium(0)-catalyzed coupling reaction of dialkoxyborane with aryl halides: Convenient synthetic route to arylboronates. *J. Org. Chem.* **62**, 6458–6459.
75. Wang, D., J. M. Schlegel and E. Galoppini (2002) Synthesis of rigid-rod linkers to anchor chromophores to semiconductor nanoparticles. *Tetrahedron* **58**, 6027–6032.
76. Abraham, R. J., M. Canton and L. Griffiths (2001) Proton chemical shifts in NMR: Part 17. Chemical shifts in alkenes and anisotropic and steric effects of the double bond. *Magn. Reson. Chem.* **39**, 421–431.
77. Hamza, K., R. Abu-Reziq, D. Avnir and J. Blum (2004) Heck vinylation of aryl iodides by a silica sol-gel entrapped Pd(II) catalyst and its combination with a photocyclization process. *Org. Lett.* **6**, 925–927.
78. Concepcion, A. B., K. Maruoka and H. Yamamoto (1995) Organoaluminum-promoted cycloaddition of trialkylsilylketene with aldehydes: A new, stereoselective approach to *cis*-2-oxetanones and 2(*Z*)-alkenoic acids. *Tetrahedron* **51**, 4011–4020.
79. Freeman, F. and J. C. Kappos (1986) Permanganate ion oxidations. 16. Substituent effects on the rate of oxidation of  $\alpha$ ,  $\beta$ -unsaturated carboxylate ions. *J. Org. Chem.* **51**, 1654–1657.
80. DiMagno, S. G., V. S.-Y. Lin and M. J. Therien (1993) Catalytic conversion of simple haloporphyrins into alkyl-, aryl-, pyridyl-, and vinyl-substituted porphyrins. *J. Am. Chem. Soc.* **115**, 2513–2515.
81. Gouterman, M. (1959) Study of the effects of substitution on the absorption spectra of porphin. *J. Chem. Phys.* **30**, 1139–1161.
82. Gouterman, M. (1961) Spectra of porphyrins. *J. Mol. Spectrosc.* **6**, 138–163.
83. Barnett, G. H., M. F. Hudson and K. M. Smith (1975) Concerning *meso*-tetraphenylporphyrin purification. *J. Chem. Soc. Perkin Trans. I*, 1401–1403.
84. Taniguchi, M., D. Ra, C. Kirmaier, E. K. Hindin, J. K. Schwartz, J. R. Diers, D. F. Bocian, J. S. Lindsey, R. S. Knox and D. Holten (2003) Comparison of excited-state energy transfer in arrays of hydrophosphyrins (chlorins, oxochlorins) versus porphyrins: Rates, mechanisms, and design criteria. *J. Am. Chem. Soc.* **125**, 13461–13470.
85. Tomizaki, K.-Y., R. S. Loewe, C. Kirmaier, J. K. Schwartz, J. L. Retsek, D. F. Bocian, D. Holten and J. S. Lindsey (2002) Synthesis and photophysical properties of light-harvesting arrays comprised of a porphyrin bearing multiple perylene-monoimide accessory pigments. *J. Org. Chem.* **67**, 6519–6534.
86. Strickler, S. J. and R. A. Berg (1962) Relationship between absorption intensity and fluorescence lifetime of molecules. *J. Chem. Phys.* **37**, 814–822.
87. Gentemann, S., C. J. Medforth, T. Ema, N. Y. Nelson, K. M. Smith, J. Fajer and D. Holten (1995) Unusual picosecond  $^1(\pi, \pi^*)$  deactivation of ruffled nonplanar porphyrins. *Chem. Phys. Lett.* **245**, 441–447.
88. Gentemann, S., N. Y. Nelson, L. Jaquinod, D. J. Nurco, S. H. Leung, C. J. Medforth, K. M. Smith, J. Fajer and D. Holten (1997) Variations and temperature dependence of the excited state properties of conformationally and electronically perturbed zinc and free base porphyrins. *J. Phys. Chem. B* **101**, 1247–1254.
89. Retsek, J. L., C. J. Medforth, D. J. Nurco, S. Gentemann, V. S. Chirvony, K. M. Smith and D. Holten (2001) Conformational and electronic effects of phenyl-ring fluorination on the photophysical properties of nonplanar dodecaarylporphyrins. *J. Phys. Chem. B* **105**, 6396–6411.